5-2018

Characterization of Type I Collagen and Osteoblast Response to Mechanical Loading

Silvia P. Canelón
Purdue University

CHARACTERIZATION OF TYPE I COLLAGEN AND OSTEOBLAST RESPONSE TO MECHANICAL LOADING

A Dissertation

Submitted to the Faculty

of

Purdue University

by

Silvia P. Canelón

In Partial Fulfillment of the

Requirements for the Degree

of

Doctor of Philosophy

May 2018

Purdue University

West Lafayette, Indiana

THE PURDUE UNIVERSITY GRADUATE SCHOOL
STATEMENT OF DISSERTATION APPROVAL

Dr. Joseph M. Wallace, Chair

Department of Biomedical Engineering,

Indiana University-Purdue University at Indianapolis

Dr. Sherry L. Voytik-Harbin, Co-Chair

Weldon School of Biomedical Engineering, Purdue University

Dr. Sarah Calve

Weldon School of Biomedical Engineering, Purdue University

Dr. Alexander G. Robling

Department of Anatomy and Cell Biology, Indiana University School of Medicine

Approved by:

Dr. George R. Wodicka

Head of Biomedical Engineering, Purdue University

This work is dedicated to my family.
Thank you for paving the way for me to carve out my own path,
create my own experiences, and embark on my own journey.

ACKNOWLEDGMENTS

I would like to begin by thanking my advisor Joseph Wallace for his invaluable mentorship over the course of my graduate career. His passion for research inspired me to push through the most challenging aspects of my work and his leadership helped cultivate confidence in me as an independent researcher. Joey, thank you for your unwavering dedication to the lab and my success as a graduate student. Your guidance has led me to this point through an extraordinary learning experience and for that I am truly grateful.

Thank you to the members of my thesis committee for their continued support throughout this endeavor, not only at the milestone meetings but at various points in between. Sherry Voytik-Harbin, Alex Robling, and Sarah Calve, thank you for serving on my committee and providing expertise as well as encouragement.

To members of the Bone Biology and Mechanics Lab, both past and present, thank you for keeping things interesting both inside and outside of the lab. The strongest element of fun during lab meetings and conferences was incorporated thanks to the energy you all brought to the table.

Will Thompson, I cannot thank you enough for the time and effort you dedicated to helping me with primary cell isolation, and for the continued support with the mechanical loading system's ups and downs. I consider myself fortunate to have had you as a mentor during the time I collected the bulk of my data and appreciate your willingness to provide your lab for whatever needs I might have had. Last, but not least, thank you for the great conversation and interest in my work and career aspirations.

Thank you to Drs. Hiroki Yokota, Chien-Chi Lin, Sungsoo Na, Jiliang Li, Teresita Bellido, and Lilian Plotkin for granting me access to a multitude of resources including lab space, equipment, and consumable materials. I would also like to thank

Catherine Whittington, Whitney Bullock, Qiaoqiao Wan, Max Hammond, Nancy Tanjung, Andy Chen, and Erin McNerny for sharing their expertise as I learned and optimized various techniques. Finally I must thank Karl Dria, Cary Pritchard, and Donna Rowskowski for their time and flexibility in granting me access to critical equipment, and for their patience in providing training.

Without Sherry Clemens, Sandy May, Tammy Siemers, and Vicki Maris my time as a graduate student would surely have been tumultuous and lacking in personal growth opportunities. Thank you for always being available to field questions and for your dedication to your work. You truly are tremendous assets to your respective universities.

I would like to extend a special thank you to Shannon Brasovan at the Practice Indie yoga studio for making it possible for me to develop a yoga practice over the past couple of years. This practice helped ground me during my most difficult professional and personal challenges and I cannot imagine my life complete without it. Shannon, I am profoundly grateful for your generosity, wisdom, light, and friendship...more than I could ever find the words to express. Having you in my life has been such a gift. Namaste.

To my husband, Matt McDermott, I offer a profound gratitude difficult to find words for. I began and ended my graduate career with him by my side and I would not have reached the level of potential I have just scratched the surface of without the journey that we have been on together. Matt, thank you for the love and companionship that have meant so much to me. Thank you for the incredible amount of support you provided, particularly in the months leading up to my defense. And thank you for the laughter and beautiful memories.

I am drawn to conclude my acknowledgments with those responsible for laying down the foundation on which I built my success. I will be eternally grateful to my parents, Dario Canelón Sr. and Soraira Suarez, not only for providing a loving home but also for making the sacrifices they did in bringing our family to the United States and securing an excellent education for their children. They set examples for the

values and work ethic that I draw on everyday and personal qualities that I hold most dear. My brother, Dario Canelón Jr., has always had my back and I cannot begin to describe how thankful I am to have had him in my corner since childhood. My sister, Claudia Canelón, has always been a source of light in my life and I feel overwhelming gratitude for her kind nature and beautiful personality. Mom, dad, Dario, and Claudia, the unconditional love and support each of you has blessed me with has helped make me who I am proud to be today, and for that I thank you from the bottom of my heart. I couldn't have gotten here without you.

TABLE OF CONTENTS

Page

Page

LIST OF TABLES

LIST OF FIGURES

Figure Page

ABBREVIATIONS

2D	Two dimensional
3D	Three dimensional
AFM	Atomic force microscopy
Ca^{2+}	Calcium
JNK	c-Jun N-terminal kinases
CDF	Cumulative distribution function
Δ-DHLNL	Dehydro-dihydroxylysinonorleucine
ΔHLNL	Dehydro-hydroxylysinonorleucine
ΔLNL	Dehydro-lysinonorleucine
DHLNL	Dihydroxylysinonorleucine
DN-VC	DN-vector control
ECM	Extracellular matrix
ERK	Extracellular signal-regulated kinases
FFT	Fast-fourier transform
FSS	Fluid shear stress
FT	Fourier transform
HLKNL	Hydroxylysino-ketonorleucine
HLNL	Hydroxylysinonorleucine
HP	Hydroxylysyl pyridinoline
HPL	Hydroxylysyl pyrrole
LRP5	Lipoprotein receptor-related protein 5
LKNL	Lysino-ketonorleucine
LNL	Lysinonorleucine
LP	Lysyl pyridinoline

LPL	Lysyl pyrrole
mRNA	Messenger RNA
MAPK	Mitogen-activated protein kinases
MC3T3-E1	Murine osteoblasts
NAD+	Nicotinamide adenine dinucleotide
NO	Nitric oxide
OCN	Osteocalcin
OI	Osteogenesis imperfecta
OPN	Osteopontin
OVX	Ovariectomy
PPFF	Parallel-plate fluid flow
PBS	Phosphate buffer saline
PMMA	Poly (methyl methacrylate)
PGE_2	Prostaglandin E_2
SEM	Scanning electron microscopy
SSV	Serial surface view
SAXS	Small-angle x-ray scattering
TEM	Transmission electron microscopy
WT	Wild type

ABSTRACT

Canelón, Silvia P. Ph.D., Purdue University, May 2018. Characterization of Type I Collagen and Osteoblast Response to Mechanical Loading. Major Professor: Joseph M. Wallace.

Bone is a composite material made up of an inorganic (hydroxyapatite mineral) phase, a proteinaceous organic phase, and water. Comprising 90% of bones organic phase, type I collagen is the most abundant protein in the human body. Both hydroxyapatite and collagen contribute to bone mechanical properties, and because bone is a hierarchical material, changes in properties of either phase can influence bulk mechanical properties of the tissue and bone structure.

Type I collagen in bone is synthesized by osteoblasts as a helical structure formed from three polypeptide chains of amino acids. These molecules are staggered into an array and the resulting collagen fibrils are stabilized by crosslinks. Enzymatic crosslinking can be limited by compounds such as -aminopropionitrile (BAPN) and result in a crosslink deficiency characterizing a disease known as lathyrism. BAPN acts by irreversibly binding to the active site of the lysyl oxidase enzyme, blocking the formation of new crosslinks and the maturation of pre-existing immature crosslinks.

Understanding how changes in bone properties on a cellular level transcend levels of bone hierarchy provides an opportunity to detect or diagnose bone disease before disease-related changes are expressed at the organ or tissue level. This dissertation studies the *in vitro* effect of BAPN-induced enzymatic crosslink reduction on osteoblast-produced collagen nanostructure, mechanical properties, crosslink ratio, and expression of genes related to type I collagen synthesis and crosslinking. The work also explores the effect of mechanical loading via applied substrate strain on these properties to investigate its potential compensatory impact.

1. REVIEW OF TYPE I COLLAGEN CHARACTERIZATION

Review of Type I Collagen Characterization

Osteoblast-produced collagen found in the extracellular matrix of skeletal tissues has been studied in an attempt to determine how its biochemical, structural, and functional properties differ between healthy and diseased tissue and change in response to external stimuli. Some studies have observed tissue-level changes in collagen induced by mechanical stimulation, others have focused on the osteoblast response to mechanical stimulation, and a small number of studies have investigated properties of collagen *in vitro*. In addition, the studies that aim to establish a correlation between nano-/microscale properties of collagen and macroscale properties of bone have not consistently shown any trend. To date, there is no clear evidence of how changes in nano-/microscale collagen properties can transcend bone hierarchy and impact the macroscale bone phenotype. In order to begin filling this knowledge gap, the properties of collagen produced by osteoblasts *in vitro* should be investigated, in particular as they relate to disease and mechanical stimulation.

1.1 Background

Bone as a type of skeletal tissue is a composite material made up of a hydroxyapatite inorganic (mineral) phase, a collagenous/non-collagenous protein organic phase, and water. The collagen comprising most of the organic phase, type I collagen, is the most abundant collagen of the human body. It is found not only in bone, but in connective and muscular tissue as well. Hydroxyapatite and collagen contribute to bone mechanical properties; hydroxyapatite provides compressive strength and stiffness to the material while collagen provides tensile strength and ductility. Because bone is

a hierarchical structure as indicated in Fig. 1.1, changes in the properties of either phase can influence bulk mechanical properties of the bone which in some cases can compromise the bones ability to serve its structural function of bearing dynamic loads associated with movement. For example, decreased bone strength is characteristic of osteoporosis and reflects deterioration in bone density and bone quality. Osteogenesis imperfecta, also known as brittle bone disease, is also characterized by decreased bone strength, and is caused by disruptions in the structure or amount of type I collagen.

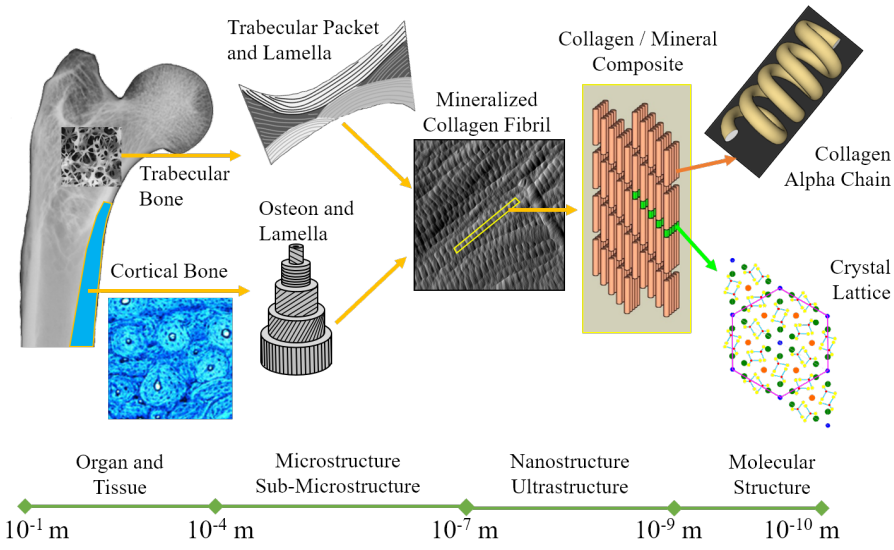

Fig. 1.1. **Hierarchical structure of bone**. Image used with permission from Joseph Wallace.

In response to dynamic loading of the musculoskeletal system, bone undergoes mechanical adaptation by continually modifying its mass and architecture via two processes: modeling and remodeling. Modeling shapes bone and increases bone mass, particularly during skeletal development, while remodeling renews bone. These processes are carried out on a cellular level by primarily three cell types: osteoblasts which synthesize bone matrix, osteoclasts which resorb bone, and osteocytes which act as mechanical sensors and produce signals to activate osteoblasts, osteoclasts, or their progenitors.

Understanding how changes in bone properties on a cellular level transcend levels of bone hierarchy provides an opportunity to detect or diagnose bone disease before disease-related changes are expressed at the organ or tissue level. Specifically, it is important to understand which collagen matrix properties are consistent between early and late stages of development and which are modified in response to an external stimulus.

1.2 Literature Analysis Approach

The literature analysis was performed using primary publications relating to bone biology and mechanics using a combination of the following major keywords to narrow the selection: type I collagen, osteoblasts, mechanical stimulation, *in vitro* collagen, and collagen structure. Articles were found using PubMed and Google Scholar, and retrieved using the Purdue University and Indiana University-Purdue University at Indianapolis library journal subscriptions. Mendeley desktop and web tools were used to store, organize, and reference relevant publications. Literature was organized into biochemical, structural, and functional collagen analyses sections as well as one dedicated to mechanical stimulation of osteoblasts.

1.3 Biochemical Analysis

Biochemical properties of collagen can be determined using various assays including analysis of $\alpha 1$ and $\alpha 2$ chain structure and quantity; quantification of procollagen peptides (N-telopeptides and C-telopeptides); analysis of amino acids such as hydroxyproline; among others [1–4]. However, the most widely used method of analysis involves quantification of collagen crosslinks. This analysis will be the focus of this review, particularly as it relates to bone material properties.

1.3.1 Collagen crosslinking

In order to evaluate the nanoscale structural aspects of bone across its hierarchy, the morphometry and organization of its constituents, mainly collagen, must be analyzed. The procollagen molecule synthesized by the cell is a helical structure formed from three polypeptide chains of amino acids. Each chain is a left-handed helical structure with repeating Gly-X-Y triplets where Gly is glycine, X is usually proline, and Y hydroxyproline [5]. In type I collagen, two of these polypeptide chains are $\alpha 1$ helices and one is an $\alpha 2$ helix. The N and C terminal ends of these polypetides are cleaved extracellularly by N and C proteinases, respectively, forming a tropocollagen molecule with telopeptide ends. These molecules self-assemble in line with one another into microfibrils, then in parallel into quarter-staggered arrays with overlap and gap regions, and finally into three-dimensional fibrils as shown in Fig. 2.1 at a later point. These fibrils are stabilized in their staggered array within a fibrillar structure by intrafibrillar and interfibrillar crosslinks, respectively [6–8].

These enzymatic crosslinks can be categorized into immature and mature crosslinks where mature crosslinks are formed from immature crosslinks [8]. Enzymatic crosslink formation begins with telopeptide lysine and hydroxylysine precursors which, through lysyl oxidase initiation, convert to telopeptide aldehydes, allysine and hydroxyallysine, respectively. These aldehydes, in combination with other precursors (i.e. helical lysine, helical hydroxyline), form immature crosslinks, some of which turn into mature crosslinks, as shown in Fig. 1.2. Pyrroles and pyridinolines are predominantly found in bone whereas only pyridinolines are found in cartilage [8]. Immature crosslinks convert spontaneously into mature crosslinks with aging and can be modified in disease states [8, 9]. Crosslink formation is possible only at specific locations, requiring the molecules to be positioned in a particular orientation relative to one another. It is important to quantify collagen crosslinks in bone because they serve as indicators of new collagen synthesis, such as in bone repair, or lower bone turnover as occurs with aging [8].

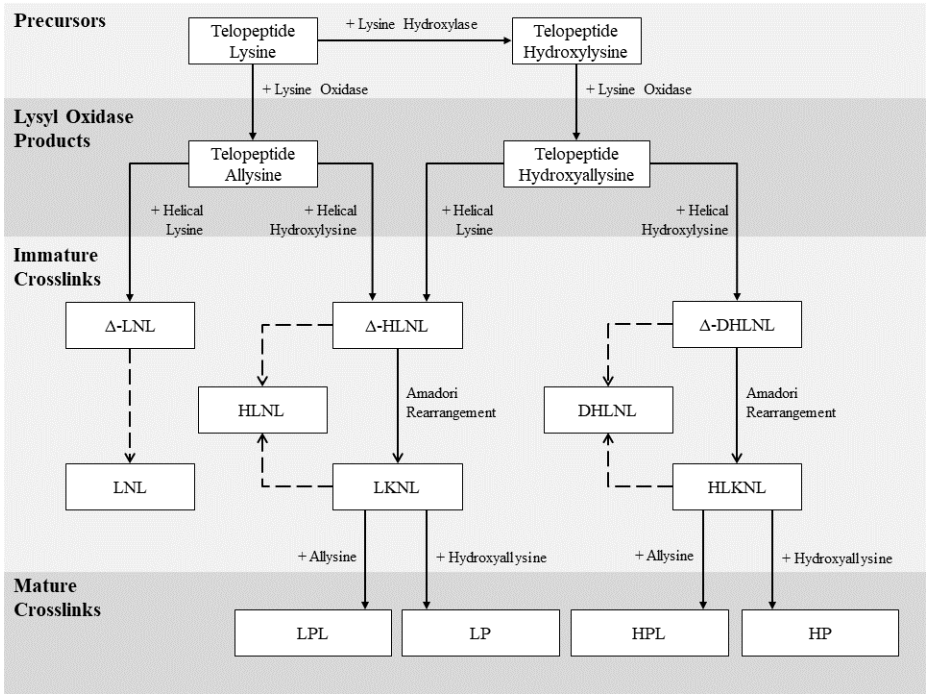

Fig. 1.2. **Chemical pathway of enzymatic collagen crosslink formation in bone**. Solid arrows with solid arrowheads indicate reactions, solid arrows with open arrowheads represent an Amadori rearrangement, and dashed arrows with open arrowheads represent a borohydride reduction required to stabilize crosslinks for identification and subsequent quantification. Adapted from Eyre *et al.* [8] and Saito *et al.* [10].

Other enzymatic mature crosslinks such as histidinohydroxylysinonorleucine and non-enzymatic crosslinks such as advanced glycation end-products (i.e. pentosidine) also play an important role in collagen stability, but will not be addressed in this review. OI has four main severity levels caused by mutations in the *COL1A1* or *COL1A2* genes, and many others sublevels caused by other gene defects [11–13]. The disease is characterized by brittle bones resulting from decreases in collagen quantity and/or quality within the collagenous matrix [14]. Vetter *et al.* [15] and, more recently, Bank *et al.* [14] studied crosslinking in bones of OI patients with disease severity levels type I, III, or IV. Vetter *et al.* found no difference in levels of HP or LP individually, or as a ratio (HP/LP), between diseased and healthy bone. This

was also true in the Bank *et al.* study though a higher level of HPD was seen with diseased bone. In addition, no correlation was found between crosslink levels and OI phenotypic severity level. The studies were done to determine if lower levels of crosslinks are responsible for disorganized collagen packing and the results suggested that the packing geometry of collagen was not altered in the OI bone. These collagen crosslinks, along with mechanical properties, were studied by Silva *et al.* in type I diabetic bone with induced osteopenia [16]. Monotonic three-point-bending of ulnae and femora showed that only structural (rigidity, yield/ultimate moments, and energy-to-fracture) as opposed to material (modulus and yield/ultimate stress) properties decreased significantly in the diabetic group relative to the control. Fatigue life data also showed that diabetic bones were significantly different from control bones in terms of structural rather than material properties. LP levels were significantly lower in diabetic bones relative to the control and HP levels did not differ. No direct correlation between crosslinking and mechanical properties was made, so whether biochemical properties of diabetic osteopenic bone contributed to its weakened mechanical properties remained unclear.

Contrary to Silva *et al.* [16], Viguet-Carrin *et al.* attempted to correlate crosslink concentration to mechanical properties but was unsuccessful [17]. Advanced glycation end-product formation was induced *in vitro* using ribose, and three-point bending tests were performed on the treated cortical bone samples to extract a variety of material properties. None of these properties were found to correlate to HP or LP concentrations. In a previous study, Viguet-Carrin *et al.* performed compression tests on human lumbar vertebrae to determine if structural properties were related to enzymatic crosslink concentrations [18]. The results showed no correlation between mechanical properties and the concentration of HP or LP. A similar study published the same year by Garnero *et al.* was successful at finding this correlation in femoral bone [19]. Three-point bending data as well as compression data revealed a significant correlation between HP concentrations and all of the extracted material properties: negative for bending modulus, bending yield stress, compressive modulus, compres-

sive yield stress, and ultimate stress, and positive for toughness. Correlations were seen to a lesser extent with LP concentrations. Given the large difference in scale between molecular crosslinking and whole bone mechanical properties, Hernandez *et al.* explored a smaller scale and tested individual trabeculae, from human vertebrae, in tension [20]. No correlation was found between any material property extracted from the mechanical test and the concentrations of HP, LP, or their combination. Overall, no consistent correlation between crosslink concentrations and mechanical properties has been found.

In addition to mature HP and LP crosslinks, Banse *et al.* also quantified mature HPL and immature HLNL and DHLNL crosslinks [21]. Compression tests were performed, as in similar studies [22] to extract material properties (modulus, strength, and strain-to-failure); however, cored cylindrical samples were tested instead of the entire vertebral body. Even with this change in methods, no individual concentrations of immature or mature crosslinks were found to be correlated with any mechanical property. The ratio of HP to LP (HP/LP), though, was found to be positively correlated with modulus and strength to a statistically significant degree. HP, LP, and HPL, in relation to mechanical properties, were also studied by Knott *et al.* in avian humeri and tibiotarsi [23]. Three-point bending failure stress was negatively correlated with HP/LP and HPL in the humerus, while compressive failure was found to be positively correlated with HPL in the tibiotarsus. A new approach was taken by Banse *et al.* in a study investigating the relationship between both immature and mature enzymatic crosslinks and morphometric measures of bone [24]. Only the ratio HPL/HP showed any correlation to morphometric measures; it was negatively correlated to trabecular spacing, trabecular number, and trabecular thickness.

Together, these studies explored the majority of the major immature and mature bone crosslinks. Crosslinks are examined independently and in combination, and in relation to a variety of properties including disease phenotypes, structural properties, material properties, and morphological properties. There is no consistent relationship between crosslinking at the molecular level and physical properties at the tissue level.

This lack of a strong correlation is not surprising given that bone is a hierarchical structure and the disparity in length scale at which biochemical and physical properties are studied and quantified. The need for the investigation of collagen properties at a molecular, nano- and microscale, is evident; the study of collagen synthesized in its native state would be beneficial in filling this gap.

1.4 Structural Analysis

As mentioned previously, collagen is organized into a quarter-staggered array where the overlap and gap regions produce an oscillating topography of axially repeating bands along the fibril length; these bands are called the D-spacing or periodicity and are generally measured around 67nm as highlighted in Fig. 2.1 [25, 26].

Morphometric characteristics of collagen such as the fibril diameter and axial periodicity have been measured using multiple methods, the most prominent being AFM which receives primary focus in this review.

1.4.1 D-spacing analysis and fibril diameter

One of the primary ways in which type I collagen is morphologically characterized is by measurement of fibril D-spacing and diameter. The comparisons of these two measurements provide a way to detect differences in collagen structure across tissue types and disease. Both morphometric characteristics have been visualized using AFM: some studies only measured fibril diameter [27, 28], others measured only D-spacing [29–33], and a number measured both [28, 32, 34–40]. Of these studies that measured both characteristics, the following mainly focused on evaluating fibril morphology and will give an idea of the kind of differences seen between tissues. Ge *et al.* used both AFM and TEM to compare collagen fibril morphology of dehydrated mineralized and demineralized wild type zebrafish vertebral bone [28]. Areas of the bone were found to have fibrils with the characteristic D-spacing and larger fibril diameters were associated with mineralized samples. In this case, samples were

processed for imaging and measurements were made manually by use of software tools. When examining dehydrated ivory and bovine dentin and bone, Bozec *et al.* also made measurements manually, but made use of FT to measure periodicity for comparison purposes [35]. Periodicity between dentin and cortical bone was comparable but fibril diameter was greater in dentin samples. In addition, periodicity measured by FT was lower than that measured manually, but not significantly so. Dentin (human) was also studied by Habelitz *et al.*, in order to compare hydrated vs. dehydrated samples [36]. Interestingly, this study was one of the first to consider presenting the data as a distribution. While both sample groups showed similar diameter ranges, hydrated samples should narrower diameter distributions compared to those of dehydrated samples. As for the periodicity, both the range of values and their distribution were similar between dehydrated and hydrated samples (data summary provided in Table 2.1). These studies were thorough in making measurements, but it is important to recognize the limitations of the methods employed. Overall, most of the studies made D-spacing measurements directly off of the computer screen using measurement tools of the available software. As with any kind of manual measurement, measurement error is introduced by the user each time boundary points are selected. This is important to consider when analyzing AFM images because said boundaries (i.e. gap and overlap bands, fibril borders) are often hard to distinguish. This becomes particularly difficult when the collagen is mineralized and the mineral obstructs the underlying collagen fibril, or when neighboring fibrils overlap and their lateral boundaries are not clearly shown. To help eliminate some of the error introduced with D-spacing measurements, more recent studies (reviewed next) make use of FT analysis. As far as sample preparation is concerned, studies which fixed and/or embedded the samples [28] were not able to measure true properties because collagen is no longer in its native environment once it has been processed. Fibril diameter as a morphological measure of type I collagen has been studied extensively, but cannot be reliably measured, let alone be used to detect statistical differences between tis-

sue types.As evidenced by the studies summarized in Table 2.1, average values for D-spacing are generally reported without explanation.

[28] [35] [36] Traditionally, distributions in D-spacing have been attributed to noise and only recently have they have been statistically analyzed and found capable of detecting differences between tissue types. The sub-section to follow discusses these recent studies.

D-spacing as distribution

Wallace *et al.* conducted the first published study looking at type I collagen D-spacing as a distribution, by analyzing histograms and their corresponding CDF [41].CDFs show what fraction of the sample is found at each D-spacing value and can be statistically analyzed with a Kolmogorov-Smirnov or Anderson-Darling test. Morphology of bone from three different animals was compared: mice (femur), sheep subjected to an OVX procedure (radius), and sheep subjected to a sham surgery (radius). The ovariectomy procedure caused an estrogen deficiency which was allowed to develop over the course of two years, and thus provide an osteoporosis disease state. Images of collagen were acquired in air and analyzed using 2D-FFT to obtain the first harmonic of the periodic spectrum (highest peak), which corresponds to the D-spacing. No significant difference was seen in mean collagen D-spacing between mice and sham-surgery sheep. In contrast, a significant difference in the mean was seen between OVX-sheep and sham-sheep collagen. As alluded to earlier, the approach used in this study has had a strong impact in the field of bone morphology because it compares D-spacing distributions (in addition to mean values) allowing the detection of a change or difference in collagen structure. To this point, a significant difference in D-spacing distribution was also found between collagen of OI and WT mouse bone in a separate study by Wallace *et al.* [42] These results were also found to be true by Kemp *et al.* when comparing OI and WT mouse tendon in both hydrated and dehydrated conditions [43]. These studies pave the way for statistically sound

Table 1.1.

Collagen fibril measurements.Demineralized indicates whether the sample was removed from the imaged surfaced; Fluid/Air indicates whether the image was taken in fluid or air; all Fibril D-spacing measurements were made manually unless otherwise noted (i.e. FT). Values recorded by Habelitz *et al.* correspond to peaks seen on a line graph of Frequency vs. D-spacing/Diameter.

Reference	**Sample**	**Demineralized**	**Image**	**Fluid/Air**	**Fibril D-Spacing (nm)**	**Fibril Diameter (nm)**
Ge [28]	Zebrafish	No	AFM	Air	63.3 ± 5.3	167.2 ± 6.8
		Yes	AFM	Air	66.6 ± 3.8	83.2 ± 5.4
		No	TEM	Air	Not evident	85.8 ± 5.3
		Yes	TEM	Air	65.3 ± 2.3	80.6 ± 6.5
Bozec [35]	Ivory or bovine dentin	No	AFM	Air	69.4 ± 4.3	140.6 ± 12.4
	Ivory or bovine cortical bone	No	AFM	Air	66.5 ± 1.4	62.2 ± 7
	Ivory or bovine cortical bone	No	AFM	Air	64.1 (FT)	N/A
Habelitz [36]	Human dentin	Yes	AFM	Air	57, 62, 67	80-105
		Yes	AFM	Fluid	67, 68	83, 91, 100

analyses of collagen fibril morphology in diseased collagen-based tissues. D-spacing distributions also serve to detect differences in collagen originating from different tissues. Wallace *et al.* compared collagen from mouse tendon, teeth, and femoral bone and found that while average D-spacing was similar across types, the distribution of D-spacing measurements from each was statistically different from that of the others [44]. Erikson *et al.* analyzed D-spacing distributions of hydrated and dehydrated paired samples of bovine skin [45] and found no significant difference between hydration states [36]. The 2D-FFT approach was also applied by Erikson *et al.* to analyze data from other studies: SEM images of human Achilles tendon [46] and SAXS data from turkey tendon [47]. A distribution was found in both human and turkey tendon, and the distribution magnitude found in the turkey tendon was similar to that shown in the SAXS analysis. D-spacing distributions have proven useful in detecting differences between healthy and diseased collagen as well as between tissue types but have not been used to study morphology of *in vitro* produced collagen. The only studies that have even looked at D-spacing of collagen *in vitro* have examined purified or processed collagen as seen in the following studies.

In vitro collagen assembly and synthesis

In contrast to tissue-level collagen morphology, *in vitro* cell-produced collagen morphology has not been studied in detail and the studies reviewed in this subsection only briefly examine morphological properties. Goh *et al.* conducted a time-course study of *in vitro* assembly of purified dermal calf collagen [48].D-spacing was evident in the AFM images of collagen, though no D-spacing measurements were made. Another time-course study of *in vitro* collagen assembly was performed by Gale *et al.* to determine how fibril length and diameter changed by means of axial or lateral interactions throughout early steps of fibrillogenesis [49]. Fibrils within the first thirty minutes were 1-2nm in diameter, while those measured within the following thirty minutes were 2-6nm. D-spacing was measured to be $\sim$67nm and all

measurements were made manually using available software. Thurner *et al.* [33] and Barragan-Adjemian *et al.* [34] induced *in vitro* collagen synthesis by preosteoblastic and preosteocytic cells, respectively, but neither study made any D-spacing or diameter measurements. Moreover, the collagen produced in both of these studies was fixed prior to AFM imaging. The nature of these studies and the *in vitro* assembly studies does not allow for evaluation of collagen in its native state: post- cell secretion, non-purified, and non-processed.

1.5 Functional Analysis

As mentioned in past sections of this review, mechanical properties are important metrics in collagen characterization. Mechanical properties at the nano- or micro-scale level can be extracted using AFM by pushing or pulling collagen fibers. Pushing, or indenting, is the more well-established method and receives most of the attention in this section. Pulling is only discussed in terms of mechanical characterization *in vitro*. The properties obtained in the following studies include the indentation modulus, indentation depth, energy dissipation, and adhesion force.

AFM indentation was performed by Grant *et al.* on hydrated or dehydrated collagen fibrils prepared from bovine Achilles tendon [50]. A three order of magnitude difference was seen in elastic modulus of the dehydrated vs. hydrated sample; dehydration caused an increase in modulus. The same trend was observed by Kemp *et al.* when indenting collagen of hydrated and dehydrated OI and WT mouse tendon [43]. The study used CDFs, as other studies have [41, 42, 44], to examine differences in indentation modulus, indentation depth, energy dissipation, and adhesion force. The adhesion force was found to differ significantly between dry OI and WT tendon, and a strong positive correlation was found between adhesion force and energy dissipation for both phenotypes. This was also true of wet tendon, and modulus and indentation depth were also seen to differ significantly between the two phenotypes. Differences in mechanical properties of hydrated vs. dehydrated collagen fibrils was confirmed

by Gautieri *et al.* using in silico molecular dynamics tests [51]. Results showed that dehydrated collagen experienced tighter molecular packing.

Similar results were obtained by Cueru *et al.* when indenting hydrated and dehydrated ewe iliac bone [52]. This study attempted to correlate mechanical properties to mineral content and found a strong positive correlation between indentation modulus and the degree of bone mineralization, pointing out an important relationship. Mechanical properties as relating to mineralization were also studied by Nassif *et al.* when comparing collagen scaffolds created from rat tail tendon collagen assembled with or without hydroxyapatite [53]. The indentation modulus of the collagen scaffold was found to be lower than that of the collagen-apatite scaffold. To study nanoscale heterogeneity in bone, Tai *et al.* indented hydrated osteonal bone samples [54]. An indentation of 5μN resulted in a 40nm indentation depth; indentation modulus mapping showed nanoscale heterogeneity among bone samples from five different animals.

In contrast to these studies, Thompson *et al.* performed *in vitro* mechanical characterization of collagen when pulling individual hydrated purified fibrils from bovine Achilles tendon [55]. This was done to study energy dissipation as a function of time delay between successive pulls. When the tip retracted more than 50nm from the substrate surface, sacrificial bonds would break and reform only when the tip came within 50nm of the surface. Energy dissipation was seen to decrease more with an increase in delay between successive pulls of the collagen molecule. Gutsmann *et al.*, however, pulled on individual hydrated native collagen fibrils from rat tail tendons and saw no reformation of bonds [56].

In summary, mechanical characterization at the collagen fibril level, has been completed mostly in tendon using nanoscale forces [43, 50, 55, 56] and to some extent in bone or bone-like samples using microscale forces [52–54]. The effects of hydration and mineralization on mechanical properties have shown to be significant in tendon and bone, respectively, but have not been studied in collagen in its native state. Mechanical characterization of collagen produced *in vitro* would not only help bridge

this gap but also avoid limitations associated with harsh sample preparation and/or processing [53, 55].

1.6 Mechanical Stimulation

Bone adapts to its mechanical environment to optimize its architecture, as well as heal, through modeling and remodeling processes [57, 58]. These are carried out on a cellular level by osteocytes, osteoblasts, and osteoclasts through mechanotransduction. Mechanotransduction is a mechanism which converts a physical force into a cellular response and, in bone, consists of four primary stages, as summarized by Turner *et al.* [59]: 1) mechanocoupling which is the process of taking a mechanical force applied to the bone and transducing it into a mechanical signal perceived, on a local scale, by sensing cells such as osteocytes; 2) biochemical coupling consists of taking that mechanical signal and converting it into a biochemical response that could lead to gene expression or protein activation; 3) signal transmission which occurs via signaling molecules, such as prostaglandin E_2 (PGE_2) and nitric oxide (NO), between the sensing cells and the effector cells including osteoblasts and osteoclasts, and; 4) effector cell response which would comprise of either bone formation by osteoblasts or bone resorption by osteoclasts on a tissue level.

Bone cell *in vivo* loading conditions can be simulated *in vitro* by exposing cultured cells to controlled mechanical inputs [60–64]. These inputs are generally compressive stress, strain, or shear stress, and can be used alone, or for more complex models, in combination. Examples of these loading modalities are summarized in Fig. 1.3.

Compressive stress has been applied to bone cells seeded two-dimensionally by using hydrostatic pressure [66, 67] or by displacing a flat plate, or platen, onto cells seeded three-dimensionally [68, 69]. Bone cells have been longitudinally stretched when seeded on a substrate in uniaxial tension [70–72] as well as when seeded onto a substrate subjected to bending [73, 74].

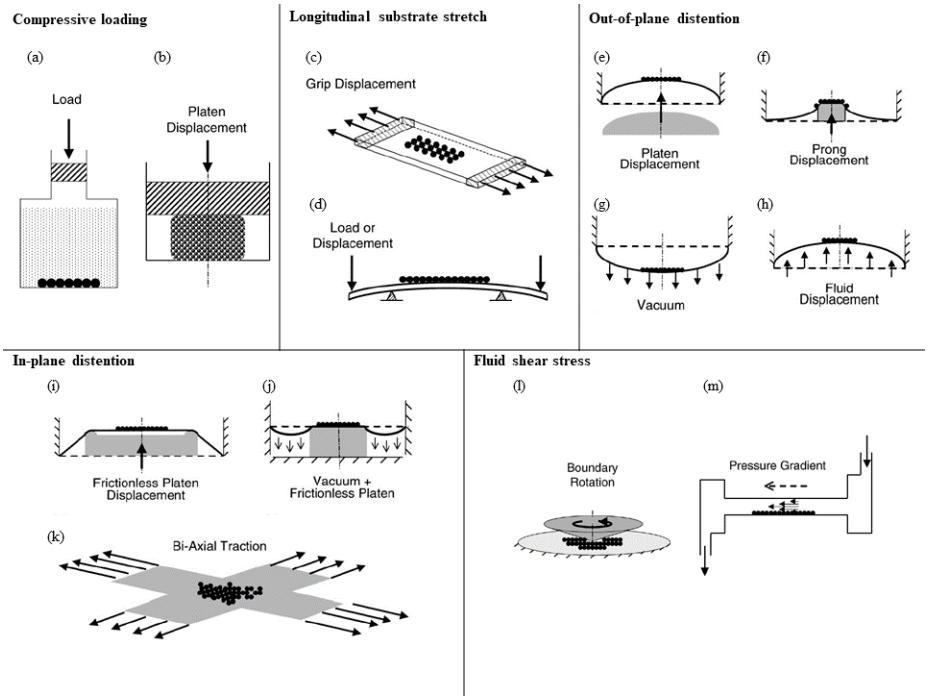

Fig. 1.3. ***In vitro* loading models**.(a) Hydrostatic pressure, (b) platen displacement onto cell scaffold, (c) uniaxial substrate stretching, (d) substrate bending, (e) positive platen displacement, (f) positive prong displacement, (g) vacuum suction, (h) positive fluid displacement, (i) positive frictionless platen displacement, (j) positive frictionless platen displacement and vacuum suction, (k) biaxial substrate stretching, (l) cone-and-plate fluid shear, (m) parallel plate fluid shear. Adapted from Brown [65].

Distention of a circular cell substrate has allowed for out-of-plane deformation by pressing the bottom of a culture dish against a convex platen [75], displacing a prong upward into the substrates [76, 77], substrate displacement via vacuum suction [78], or substrate displacement via positive fluid displacement [79]. In-plane deformation has generally been done by using frictionless platen displacement alone [80] or in combination with vacuum suction [81–84], and by biaxially stretching the substrate [85]. Fluid shear stress has been applied to bone cells using a cone-and-plate system [86] or, more commonly, a parallel plate flow chamber [87]. The latter induces fluid shear in two dimensions by pumping fluid over a layer of cells, usually by way of a

parallel-plate fluid flow (PPFF) chamber which houses a slide seeded with adherent cells. This chamber connects inline to a pumping mechanism and media reservoir which together allow the delivery of fluid in various profiles and frequencies [88]. Fluid can also be passed through a three-dimensional construct using a similar set-up with a modified chamber [89]. Recent and more complex *in vitro* mechanical loading chamber designs incorporate both fluid flow and substrate deformation [90].

As mentioned in the main introduction to this review, osteoblasts are the cells responsible for producing type I collagen the primary protein of bones organic phase which provides bone its tensile strength and ductility. For this reason, it is important to study the osteoblast response to mechanical loading, in particular as it relates to the mechanical properties of its extracellular matrix proteins, namely collagen. For bone formation to occur, osteocytes need to sense a mechanical signal and recruit osteoblasts to the bone surface. Once attached, the osteoblasts begin synthesizing the unmineralized organic component of bone known as osteoid, which eventually mineralizes to form bone [91]. In this environment, osteoblasts are exposed to bone tissue surface strains and extracellular fluid movement which serve to mechanically stimulate the cells and trigger specific intracellular signaling events, some of which are highlighted in the Fig. 1.4 diagram displaying communication between osteocytes, osteoblasts, and osteoclasts. Osteoblasts have been shown to respond to fluid shear stress and substrate strain, with PPFF and substrate distention being two of the most common applications, respectively.

Some applications of PPFF have studied the effect of flow on different types of bone cells [82, 92–94] and have evaluated their response to various loading profiles in terms of cell metabolism [94], cell signaling molecules [92], and cell signaling pathways [93, 95], but few published studies have examined collagen properties.

Zhou *et al.* compared levels of NAD+/NADH between Stat3 knockout (diseased) osteoblasts and WT osteoblasts in response to oscillatory fluid shear stress [94]. While the study focused on a disease state affecting bone morphology, the opportunity to study the effect of PPFF on bone matrix or cellular properties/activity was missed.

Jacobs *et al.* investigated differences in intracellular Ca^{2+} levels in response to three different flow profiles (steady, oscillatory, and pulsatile) and frequencies (0.5-2.0Hz) [88]. Sharp *et al.* loaded rat bone marrow stromal cells under similar fluid shear conditions to study the effect of varying pulsatile flow on bone ECM proteins [96]. Gene expression of collagen type I $\alpha 1$, OPN, bone sialoprotein, and OCN were evaluated in response to steady and pulsatile flow. Other studies examining bone matrix protein expression in response to fluid shear stress included those conducted by Wu *et al.* [97] and Barron *et al.* [89].

Substrate strain studies commonly use the widely commercially available Flexcell tension system to apply strain to cells grown in vitro. Osteoblast-like cell response to substrate strain has mostly focused on short-term outcomes of cyclic loading, including cell proliferation, metabolism [98], differentiation [99], and mechanotransduction pathways [82, 100], rather than long-term effects on collagen properties.

Neidlinger-Wilke *et al.* found a reduction in osteoblast proliferation on the silicone Flexcell plate substrate compared to plastic dishes, and similar morphology, alkaline phosphatase activity, and protein levels [98]. Increased alkaline phosphatase activity as well as matrix mineralization was confirmed in cyclically loaded mesenchymal stem cells cultures [101] though no matrix properties were assessed. When assessing multiple strains, Liu et al. determined that gene expression of type I collagen increased at 5% strain but, again, properties of the collagen produced were not evaluated in response to cyclic loading [82]. In an effort to elucidate the bone formation process, other studies showed specific integrins at the cell-ECM interface to respond to substrate strain and play a role in mechanotransduction; however, collagen properties were not included in the scope [100].

It is clear that the study of osteoblasts in response to loading, particularly relating to bone disease, and a tie between macroscale phenotypic properties and nano- or microscale properties is missing. In addition, published data shows inconsistency in collagenous protein synthesis by osteoblasts in response to loading [89, 96, 97]. Consistency is seen only with expression/synthesis of non-collagenous OPN protein which

plays a role in the mineral, rather than organic, phase of bone. In order to determine how changes in both phases at a cellular level transcend levels of bone hierarchy up to the tissue level, structural and mechanical characterization of osteoblast-synthesized collagen is required. Properties of osteoblast-synthesized collagen in response to flow would also help provide an understanding of the effects of mechanotransduction seen during bone modeling and remodeling.

1.7 Conclusions

The literature review revealed that attempts to relate collagen properties at a molecular or cellular level to those on at the tissue level have yielded inconsistent results. The lack of a strong relationship between these biochemical, structural, and functional properties on different length scales speaks to the importance of thoroughly investigating collagen properties on a nano- or microscale. In addition, the study of the effect of mechanical stimulation has been limited to macroscale properties or else to non-structural and non-mechanical microscale properties. Biochemical, structural, and functional characterization of the osteoblast-produced collagen matrix would address the knowledge gap of how bone formation processes modify bone properties at the cellular level before being reflected in higher levels of bone hierarchy and change in response to mechanical stimuli. Characterization of the osteoblast-produced collagen, in its native state, can be completed by using various assays to analyze the collagen secreted by pre-osteoblasts differentiated into osteoblasts. These assays can be used to detect differences between loaded and non-loaded states as well as disease states (i.e. osteoporosis, osteogenesis imperfecta, osteolathyrism). Modifications could be made to the already established methods employed in the studies analyzed in the literature review to analyze *in vitro* produced collagen: High performance liquid chromatography and mass spectroscopy or Fourier transform infrared spectroscopy to quantify enzymatic collagen cross-links, atomic force microscopy coupled with Fourier Transform analysis to determine collagen D-spacing, atomic force microscopy indentation

to extract collagen mechanical properties, and reverse transcription polymerase chain reaction to examine molecular signaling.

Induced and detected changes in collagen characteristics due to mechanical stimulation as attained by loading cells with fluid shear conditions analogous to those found *in vivo* requires investigation. It can be hypothesized that mechanical loading via fluid flow has the potential to recover biochemical, structural, and functional characteristics of diseased osteoblast-produced collagen at the nano- or microscale and, thus, prevent propagation disadvantageous properties to macroscale levels of bone hierarchy. The clinical implications of this understanding include providing an opportunity for diagnosis of bone disease before tissue-level function is compromised and assessing mechanical loading as treatment tool to recover advantageous properties.

2. β–AMINOPROPIONITRILE-INDUCED REDUCTION IN ENZYMATIC CROSSLINKING CAUSES *IN VITRO* CHANGES IN COLLAGEN MORPHOLOGY AND MOLECULAR COMPOSITION

2.1 Abstract

Type I collagen morphology can be characterized using fibril D-spacing, a metric which describes the periodicity of repeating bands of gap and overlap regions of collagen molecules arranged into collagen fibrils. This fibrillar structure is stabilized by enzymatic crosslinks initiated by lysyl oxidase (LOX), a step which can be disrupted using β-aminopropionitrile (BAPN). Murine *in vivo* studies have confirmed effects of BAPN on collagen nanostructure and the objective of this study was to evaluate the mechanism of these effects *in vitro* by measuring D-spacing, evaluating the ratio of mature to immature crosslinks, and quantifying gene expression of type I collagen and LOX. Osteoblasts were cultured in complete media, and differentiated using ascorbic acid, in the presence or absence of 0.25mM BAPN-fumarate. The matrix produced was imaged using atomic force microscopy (AFM) and 2D Fast Fourier Transforms were performed to extract D-spacing from individual fibrils. The experiment was repeated for quantitative reverse transcription polymerase chain reaction (qRT-PCR) and Fourier Transform infrared spectroscopy (FTIR) analyses. The D-spacing distribution of collagen produced in the presence of BAPN was shifted toward higher D-spacing values, indicating BAPN affects the morphology of collagen produced *in vitro*, supporting aforementioned *in vivo* experiments. In contrast, no difference in gene expression was found for any target gene, suggesting LOX inhibition does not upregulate the LOX gene to compensate for the reduction in aldehyde formation, or regulate expression of genes encoding type I collagen. Finally, the mature to imma-

ture crosslink ratio decreased with BAPN treatment and was linked to a reduction in peak percent area of mature crosslink hydroxylysylpyridinoline (HP). In conclusion, *in vitro* treatment of osteoblasts with low levels of BAPN did not induce changes in genes encoding LOX or type I collagen, but led to an increase in collagen D-spacing as well as a decrease in mature crosslinks.

2.2 Introduction

Bone is a composite material made up of an inorganic (hydroxyapatite mineral) phase, a proteinaceous organic phase, and water. Comprising 90% of bones organic phase, type I collagen is the most abundant protein in the human body [102] . Both hydroxyapatite and collagen contribute to bone mechanical properties; hydroxyapatite provides compressive strength and stiffness while collagen provides tensile strength and ductility [22, 103, 104]. Because bone is a hierarchical material, changes in the properties of either phase can influence bulk mechanical properties of the tissue and bone structure. In some cases, this can compromise bones ability to serve its structural function of bearing dynamic loads associated with movement. For example, decreased bone strength is a characteristic of osteoporosis and reflects deterioration in bone density and bone quality [105–107]. Osteogenesis imperfecta is also characterized by decreased bone strength and toughness, and is caused by disruptions in the quality or amount of type I collagen [12, 108, 109].

Type I collagen in bone is synthesized by mature osteoblasts as a right-handed helical structure formed from three polypeptide chains of amino acids. Each chain is a left-handed helix with repeating Gly-X-Y triplets where Gly is glycine, X is usually proline, and Y hydroxyproline [5, 110]. In type I collagen molecules, two of these polypeptide chains are $\alpha 1$ helices and one is an $\alpha 2$ helix. Once a triple-helical molecule forms, N and C terminal ends are cleaved by proteinases, leaving mature collagen molecules. These molecules self-assemble in line with one another into microfibrils, then in parallel into quarter-staggered arrays with overlap and gap regions, and finally

into three-dimensional fibrils. The overlap and gap regions produce an oscillating surface topography of axially repeating bands along the fibril length, referred to as the D-spacing or periodicity of the fibril [26] (Fig. 2.1). This D-spacing is a morphometric characteristic of collagen fibrils and exists as a distribution of values near the theoretical 67nm [25]. Changes in mean D-spacing or its distribution of values can be used to detect differences in collagen structure, tissue origin, and hydration state [41–45].

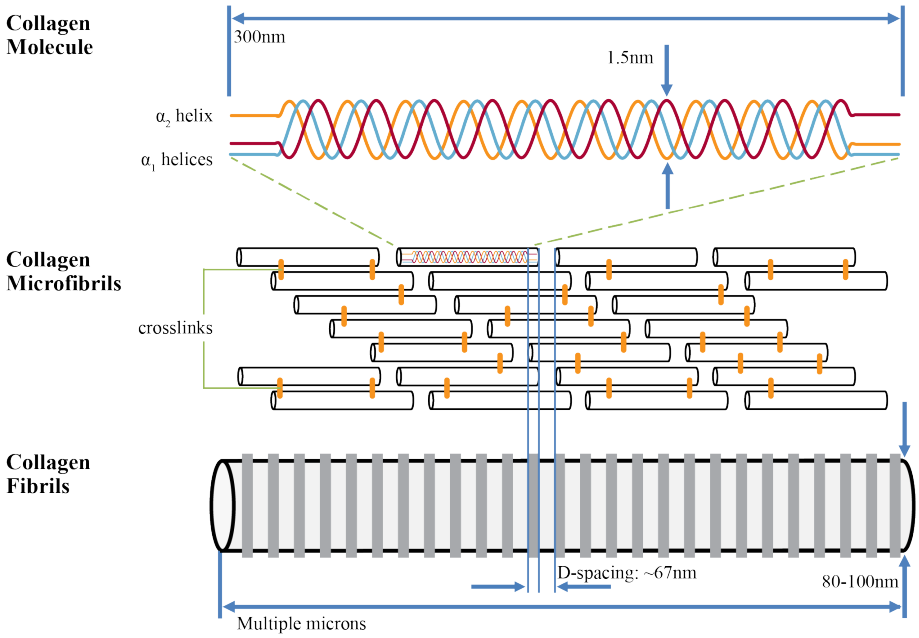

Fig. 2.1. **Collagen structure and organization**. Collagen molecules self-assemble in a quarter-staggered array into microfibrils to form collagen fibrils with characteristic periodic D-spacing. Adapted with permission from Canelón and Wallace [111]

.

Post-translationally, collagen fibrils are stabilized within their staggered array by intramolecular and intermolecular crosslinks [6, 7, 112]. Enzymatic crosslink formation begins when telopeptide lysine and hydroxylysine precursors, through lysyl oxidase (LOX) initiation, convert to telopeptide aldehydes, allysine and hydroxyally-

sine, respectively [7, 10]. The allysines, in combination with other precursors (i.e. helical lysine or hydroxylysine) form covalent chemical crosslinks. Some of these crosslinks mature to their trivalent form as pyridinolines and pyrroles. Crosslink synthesis can be limited by compounds such as penicillamine and β-aminopropionitrile (BAPN), resulting in a crosslink deficiency which characterizes a disease known as lathyrism [113–115]. BAPN is found in the seeds of the *lathyrus odoratus* plant, grown as a famine crop, and acts by irreversibly binding to the LOX active site. This binding prevents LOX from catalyzing aldehyde formation and subsequently blocks the formation of new crosslinks and the maturation of pre-existing immature crosslinks.

While BAPN has been shown to affect macroscale bone properties and nanoscale properties of type I collagen *in vivo* in rabbit, rat, and mouse models [116–118], knowledge of its direct effects on the morphology, expression, and crosslinking of collagen produced *in vitro* by osteoblasts is limited [119,120]. Evidence in the literature shows LOX mRNA expression increases with low levels of BAPN exposure, and decreases at higher concentrations as the differentiation process is impaired [120–122]. At low concentrations, as bioavailability of LOX is decreased, the cells may possess the ability to upregulate *LOX* expression to bring the level of available LOX back within a normal range. Few studies have investigated BAPN inhibition of LOX to block crosslink formation *in vitro* [119–121], and fewer still specifically attribute the effect to a change in immature or mature crosslinks [120]. The purpose of this study was to modify a key step in post-translational collagen synthesis to observe alteration to type I collagen in its native state. It was hypothesized that BAPN-induced inhibition of collagen crosslinking would (1) alter the D-spacing morphology of collagen produced *in vitro* by osteoblasts (2) drive upregulation of the LOX gene to compensate for the reduction in aldehyde formation, leading to an observed increase in mRNA expression and (3) inhibit the formation of mature crosslinks, specifically hydroxylysylpyridinoline.

2.3 Materials and Methods

2.3.1 Cell culture

MC3T3-E1 Subclone 4 (ATCC^{R} CRL-2593) murine preosteoblasts were obtained from the American Type Culture Collection (ATCC, Manassas, VA) and cultured in proliferation medium composed of αminimal essential medium (α-MEM, Life Technologies, Carlsbad, CA), 10% fetal bovine serum (FBS, GIBCO, Carlsbad, CA), 0.5% penicillin/streptomycin (GIBCO, Carlsbad, CA), and 1% L-glutamine (Hyclone, Logan, UT). MC3T3-E1 differentiation control medium consisted of proliferation medium supplemented with 50μg/ml ascorbic acid (Thermo Fisher Scientific,Waltham, MA) and differentiation experimental medium was additionally supplemented with 0.25mM BAPN-fumarate (Sigma Aldrich, St. Louis, MO) for crosslink inhibition experiments.

2.3.2 Collagen synthesis for analysis of collagen morphology

MC3T3-E1 cells were cultured in T75 flasks and allowed to proliferate for 3 days until reaching 80% confluence. Once confluent, the cells were seeded into 60mm dishes at a density of 500,000 cells per dish. Cells were seeded into eight dishes, four of them control dishes without BAPN and four treatment dishes with 0.25mM BAPN-fumarate. After seeding, the medium was replaced and supplemented with ascorbic acid for 14 days to allow differentiation and promote collagen synthesis.

2.3.3 Atomic force microscopy (AFM)

Following 14 days of differentiation, the cultures were rinsed with phosphate-buffered saline (PBS) and treated with 10mM ethylenediaminetetraacetic acid (EDTA, Life Technologies, Carlsbad, CA). Experiments in bone and tendon have shown that EDTA has negligible effects on collagen fibril morphology (data not shown) and was here used to encourage cellular detachment from the extracellular matrix (ECM) in

order to expose the newly synthesized collagen matrix for AFM imaging. After treatment with EDTA, the matrix was rinsed with ultrapurified water (Milli-Q, EMD Millipore, Darmstadt, Germany) and allowed to dry. Five locations within each dish were imaged with a Bioscope Catalyst Atomic Force Microscope (Bruker, Santa Barbara, CA) in peak force tapping mode using ScanAsyst Fluid+ probes (Bruker, Santa Barbara, CA). Within each location, a 30μm x 30μm scan area was performed to find areas where collagen was exposed by treatment with EDTA. A 10μm x 10μm scan was then performed to find suitable areas for closer examination followed by a final 3.5μm x 3.5μm scan of collagen fibrils appropriate for analysis. A 2 Dimensional Fast Fourier Transform (2D-FFT) was performed to extract D-spacing from approximately 10 individual collagen fibrils at each location, as previously described [45,123]. D-spacing analysis was performed on a minimum of 50 fibrils per dish and 200 fibrils per experimental group.

2.3.4 Quantitative reverse transcription polymerase chain reaction

An additional set of experiments was run for gene expression analysis by qRT-PCR. Cells from a single flask were seeded into ten dishes (five control and five supplemented with 0.25mM BAPN-fumarate). At the end of a 7 day differentiation period, the medium was removed from each culture dish and replaced with 1mL of TRIzol reagent (Invitrogen, CA). RNA isolation was performed using TRIzol reagent and reverse transcription (RT) was carried out using a High Capacity cDNA Reverse Transcription Kit (Life Technologies, Carlsbad, CA). PCR was performed using an ABI 7500 Fast PCR machine under the 9600 Emulation thermal cycling mode with SYBR Green primers and Power SYBR Green PCR master mix (Life Technologies, Carlsbad, CA). Primers were chosen for target genes encoding type I collagen α1 (*COL1A1*), type I collagen α2 (*COL1A2*) and *LOX* as well as reference gene β-actin (*BACT*) [124, 125]. Each sample/gene combination was run in triplicate and water was used as the no-template control. mRNA expression levels of the triplicates

were averaged. Following an efficiency-calibrated mathematical model [126], mRNA expression levels for each sample/target gene were averaged and compared to the control group using the REST^{R} program [127]. The program calculates relative expression ratios using Equation 1 and employs randomization tests to obtain a level of significance.

$$Ratio = \frac{(E_{Target})^{\Delta CT_{Target}(Control-Sample)}}{(E_{Ref})^{\Delta CT_{Ref}(Control-Sample)}} \tag{2.1}$$

E_{Target} and E_{Ref} are the qRT-PCR efficiencies of a target gene and reference gene transcript, respectively; and ΔCT is the difference in control and sample cycle thresholds for the respective gene transcript.

2.3.5 Fourier transform infrared spectroscopy (FTIR)

Following the experimental methods described above, a third set of experiments was run to analyze collagens secondary structure using FTIR. Cells were seeded into twelve dishes (six control and six supplemented with 0.26mM BAPN). After 14 days of differentiation the dishes were rinsed three times with PBS and three times with water. Samples were then directly transferred onto barium fluoride windows and air-dried.

FTIR spectroscopic analysis was performed using a Nicolet iS10 spectrometer (Thermo Fisher Scientific, Waltham, MA). A water vapor background was collected and subtracted from sample data as they were collected. Data were collected from the samples under nitrogen purge at a spectral resolution of 4cm^{-1}. A minimum of three spectra were collected per sample and they were averaged and treated as technical replicates. The amide I and amide II regions ($\sim$1400-1800cm^{-1}) were baseline corrected according to published standards [128, 129] using OriginPro (OriginLab, Northampton, MA). Underlying peaks within these regions were resolved as Gaussian peaks using second derivative analysis and each spectrum was curvefit using GRAMS/AI (Thermo Fisher Scientific, Waltham, MA). The results from the

converged peak fitting were expressed as peak position and percentage area of the peak relative to the area underneath the fitted curve. The investigation focused on peaks corresponding to positions at $\sim$1660cm^{-1} and $\sim$1690cm^{-1}, shown to be correlated to mature (HP, hydroxylysylpyridinoline) and immature crosslinks, respectively [120, 121, 130, 131].

2.3.6 Statistical analysis

All statistical analyses were performed using Statistical Analysis System (SAS Institute, Cary, NC) and a value of $p<0.05$ was considered significant for all experiments.

To investigate difference in collagen fibril morphology due to the presence of BAPN, D-spacing values measured from each culture dish were averaged to yield a single value. These mean D-spacing values from control (n=4) and treated (n=4) samples were then compared using a Mann Whitney U test. This nonparametric test was chosen due to the low sample size. To explore differences in the distribution of D-spacing values, the histogram and cumulative distribution function (CDF) of each group was generated. The distributions of the control (n=217) and treated groups (n=251) were compared using a k-sample Anderson-Darling (A-D) test as previously described [132].

Differences in mRNA expression between control and BAPN-treated samples were assessed using the REST [R] program in group means for statistical significance by using a Pair Wise Fixed Allocation Random Test [c]. The peak percentage area ratios for the FTIR experiment, were compared between the control and BAPN groups using a Students t-test.

2.4 Results

2.4.1 Atomic force microscopy

Collagen produced *in vitro* by MC3T3-E1 preosteoblasts was assessed in 60mm culture dishes. 5 distinct locations were identified and analyzed in each dish using 3.5μm x 3.5μm images (Fig. 2.2). A minimum of 10 collagen fibrils were imaged from each of 5 locations, amounting to at least 50 fibrils per dish, and totaling 217 fibril measurements for the control group and 251 for the BAPN-treated group.

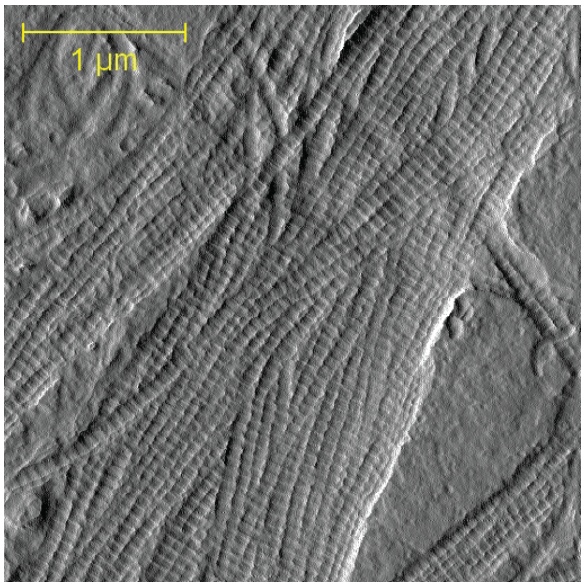

Fig. 2.2. **Representative 3.5μm x 3.5μm collagen AFM image**. AFM images of collagen in its native state were coupled with Fourier transform analysis to measure the periodic collagen fibril D-spacing.

For each dish, fibril D-spacing measurements were pooled to produce the mean D-spacing for that dish, and mean values ranged from 65.8nm to 66.8nm for the control group and from 66.6nm to 67.6nm for the BAPN-treated group. The mean D-spacing for the 4 samples was 66.4nm$\pm$0.4nm for the control group and 67.1nm$\pm$0.4nm for the BAPN-treated group ($p = 0.060$) (Fig. 2.3(B)). When all fibrils in a group were analyzed together, there was a distribution of D-spacing values ranging from 60.2nm

to 72.9nm for the control group and 61.7nm to 71.1nm for the BAPN-treated group (Fig. 2.3(a)). These distributions were significantly different from one another with the treated population shifted to higher D-spacing values over most of its range (A-D test, $p<0.0001$) (Fig. 2.3(b)).

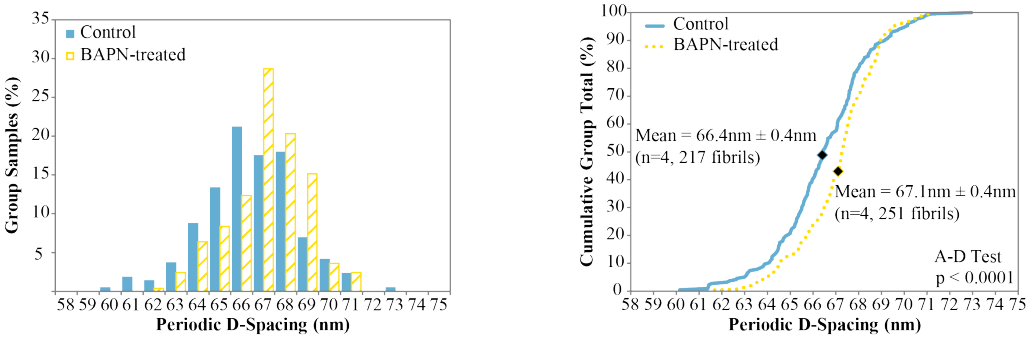

(a) Histogram

(b) Cumulative Distribution Function

Fig. 2.3. **Collagen D-spacing obtained from the D-spacing measurements in each group (n=4)**. A clear shift towards higher D-spacing values in the BAPN-treated group is evident in the (a) histogram, (b) cumulative distribution function (CDF), and mean, indicated by the diamond marks on the CDF.

2.4.2 Quantitative reverse transcription polymerase chain reaction

No significant difference was observed in the mRNA expression of any target gene in the BAPN-treated samples relative to controls (Table 2.1).

2.4.3 Fourier transform infrared spectroscopy

Peak fitting resulted in consistent peaks around 1654cm^{-1} and 1680cm^{-1} as opposed to the expected 1660cm^{-1} and 1690cm^{-1}locations. However; a positive spectral shift of $\sim$10cm^{-1} would result in positions closely matching those reported elsewhere [121, 133], therefore peaks found in this study are considered to be represen-

Table 2.1.
Fold changes in mRNA expression of BAPN-treated samples relative to controls (n=5)

Target Gene	Fold Change	Std. Error	95% Confidence Interval	p-value
COL1A1	1.011	0.759 - 1.452	0.540 - 1.562	0.966
COL1A2	1.123	0.787 - 1.447	0.616 - 1.738	0.471
LOX	1.094	0.655 - 1.931	0.448 - 2.569	0.756

tative of HP and immature crosslinks (Fig. 2.4). The spectral shift may be due to interactions with water still present in the samples after air-drying [134–136]. Treatment with BAPN resulted in a decrease in the collagen crosslink ratio driven by a significant reduction in the HP crosslink peak percent area ($p<0.05$). There was no statistical difference in the percent area of the peak corresponding to immature crosslinks (Table 2.2).

Table 2.2.
Information on underlying FTIR peaks located at $\sim$1660cm^{-1} and $\sim$1690cm^{-1}

		Mean Peak Position (cm^{-1})	Mean Peak Percent Area	Mean Area Ratio
Control	$\sim$1660 cm^{-1}	1654.3730±0.7289	16.2868±4.1089	3.9068±1.6353
	$\sim$1690 cm^{-1}	1681.0301±1.5651	4.7963±2.2037	
BAPN	$\sim$1660 cm^{-1}	1653.4087±0.9959	8.2149±3.4959	1.9865±0.6145
	$\sim$1690 cm^{-1}	1678.8092±1.0640	4.4880±2.3100	
p-value	$\sim$1660 cm^{-1}		0.0048	0.0338
	$\sim$1690 cm^{-1}		0.8177	

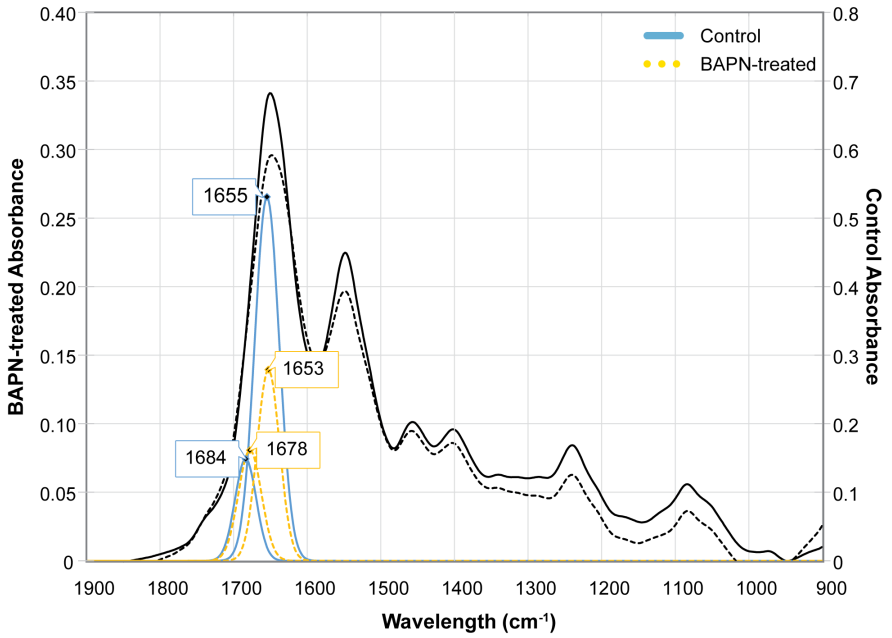

Fig. 2.4. **Representative mature and immature crosslink peak fittings underneath the FTIR spectral curve**. A decrease in the 1654cm^{-1} peak area is evident in the BAPN-treated sample relative to control. The BAPN-treated and control samples were plotted on different axes to visually highlight this difference.The black solid dashed lines correspond to the full spectra of control and BAPN-treated samples, respectively.

2.5 Discussion

It was hypothesized that BAPN treatment would cause partially differentiated MC3T3-E1 cells to synthesize a collagen matrix that was morphologically different from that produced by non-treated cells. Our data indicate that a distribution of D-spacing values, rather than a single value, exists for Type I collagen produced *in vitro* by osteoblasts. The results demonstrate that inhibition of enzymatic crosslinking via BAPN binding of lysyl oxidase causes the D-spacing distribution to shift towards higher values. D-spacing and its distribution provide information on the state and internal structure of collagen and can reflect structural defects in its α-chains or changes due to alterations in post-translational collagen synthesis. The inhibition of enzymatic crosslinking via lysyl oxidase inhibition was confirmed by the significant reduction in the mature/immature crosslink ratio and decrease in the peak percent area corresponding to HP, as a result of BAPN treatment. While analysis of D-spacing values showed a significant difference between groups, no difference was found between the control and BAPN-treated groups when comparing gene expression levels. The data showed that treatment of osteoblasts with BAPN does not induce a significant change in expression of any of the genes targeted in this study for their involvement in collagen synthesis. These results contrast those using higher BAPN concentrations in which *COL1A1* was upregulated [121] and *LOX* was downregulated [120,121] with BAPN treatment, and challenges the hypothesis that BAPN would drive upregulation of *LOX* as a response to the decrease in aldehyde formation. Results of this study highlight the effects of post-translational collagen modifications on collagen structure while demonstrating that these changes occurred in the absence of altered collagen or *LOX* gene expression.

The D-spacing distribution has been shown to be capable of reflecting differences in disease states, such as osteoporosis [41] and osteogenesis imperfecta [42,43], as well as tissue types, namely dentin, bone, and tendon [44]. The present study confirms that the D-spacing measure can capture aspects of collagen fibril structure which

may relate to the state and internal structure of individual molecules. Data revealed a significant upward shift in the D-spacing distribution between control and treatment groups. The difference in mean D-spacing had a marginally significant p value of 0.06. The low sample size (n=4) necessitated the use of a nonparametric statistical test. Given the data from the current study, a post-hoc sample size analysis indicates that a sample size of n=6 would be needed in order to detect a statistical difference between the two groups at 80% power.

The introduction of BAPN, and its binding effect on lysyl oxidase, inhibits the enzymatic crosslinking pathway preventing the formation of aldehyde products. This reduction in aldehyde products has been shown in other osteoblast studies to limit the formation of immature covalent and mature multivalent collagen crosslinks [31,39]. In addition, lysyl oxidase inhibition by a lower *in vivo* BAPN-fumarate concentration of 0.025mM was found to cause a significant shift in D-spacing in mouse bone from another study completed by our group [137]. After compensating for the added fumarate salt, this concentration corresponds to 0.0137mM BAPN, as compared with the 0.137mM BAPN concentration used in the current study. Given that this tenfold higher 0.137mM BAPN concentration corresponded to five times the half-maximal inhibitory BAPN concentration *in vivo* [138, 139], we expected greater lysyl oxidase inhibition to be induced *in vitro*. In other words, the quantitative analysis of collagen synthesized *in vitro* reflects a direct rather than systemic effect of lysyl oxidase inhibition by BAPN. The upward shift in D-spacing distribution seen in the BAPN-treated group of this study suggests that crosslinking may be responsible for compression of fibrils under normal conditions. The same trend was observed in non-mineralized collagen from mouse tail tendon in a study examining the effect of chemical fixation on mouse tail tendon [140]. In contrast, the D-spacing distribution was found to shift toward lower values in mineralized mouse bone collagen with BAPN treatment *in vivo* [137]. These differences in collagen morphology emphasize the complexity of a crosslink formation process in which *in vivo/in vitro* lysyl oxidase inhibition, bone/*de*

novo collagen synthesis, and presence/absence of mineral in the collagen matrix all play a role in allowing decompression of the collagen fibril.

Quantitative RT-PCR was used to amplify gene sequences found in RNA isolated from control and BAPN-treated osteoblasts, and to quantify mRNA expression levels. RNA was isolated from osteoblasts after seven days when collagen mRNA expression and synthesis levels were highest [141]. When comparing the two groups, the analysis of fold change in expression showed no difference in *LOX*, *COL1A1*, or *COL1A2* expression. These data indicate that inhibition of the *LOX* enzyme by 0.25mM BAPN-fumarate does not drive a significant upregulation of the LOX gene nor does it have a significant effect on the regulation of genes encoding the $\alpha 1$ and $\alpha 2$ helices that form collagen molecules. This supports other BAPN osteoblast studies in which genes encoding *LOX* were not found to be regulated at similar BAPN concentrations [120, 121]. This lack of a significant effect suggests that a 0.25mM BAPN-fumarate concentration is too low to induce osteoblasts to compensate for the lack of aldehyde formation and, consequently, collagen matrix formation and stabilization.

FTIR has been used to obtain information about protein secondary structures [128, 129], specifically as pertaining to enzymatic collagen crosslinks [134, 142]. The use of second derivative methods to locate and fit peaks underlying the FTIR spectral curve has shown a correlation between peaks at 1660cm^{-1}/1690cm^{-1} and mature/immature crosslinks [130]. Using this technique, the current study characterized the secondary structure of collagen synthesized *in vitro* by osteoblasts. Peaks were consistently found in the 1654cm^{-1} and 1680cm^{-1} regions, corresponding to mature HP and immature crosslinks, respectively. BAPN treatment resulted in a significant reduction in the HP crosslink peak percent area and decrease in the mature to immature crosslink ratio. The peak percent area of immature crosslinks was not significantly affected. Collectively, these data suggest that a 0.25mM BAPN-fumarate concentration did not inhibit the total amount of available lysyl oxidase enzyme because immature crosslinks were still present. However, the 0.25mM concentration was sufficient to prevent the maturation of divalent immature crosslinks to triva-

lent HP crosslinks. Results from this study were similar to another in which higher BAPN concentrations also caused an HP crosslink decrease [121] and differed from others which showed no change in the crosslink ratio at comparable BAPN concentrations [120]. These differences in the observed effect of lysyl oxidase inhibition on collagen secondary structure are indicative of a dose-dependent response in enzymatic crosslink formation for both immature and mature crosslinks, particularly relating to HP.

A more thorough investigation of a dose-dependent response to BAPN would elucidate the effect of lysyl oxidase inhibition on collagen gene expression and the single dosage used is considered a limitation of the present study. Consideration of other *LOX* isoforms such as *LOXL1-4* could also provide valuable information in the context of this study given that their expression could differ from that of *LOX*. Future studies will be aimed at assessing these questions and how they relate to osteoblast signaling, collagen production, and post-translational modification.

2.6 Conclusions

In conclusion, collagen synthesized in vitro by pre-osteoblastic cells was found to be fibrillar and organized in a manner to produce natural variation in its periodic D-spacing. Although there were no differences in the expression of genes relating to collagen synthesis or enzymatic crosslink initiation, partial lysyl oxidase inhibition at low levels of BAPN still resulted in significant morphological and crosslinking changes in collagen. Collagen fibrils of the BAPN-treated group were found to be morphologically different from those of the control group as seen by the significant increase in the D-spacing distribution of the BAPN-treated collagen fibrils. In addition, the ratio of mature to immature crosslinks was found to decrease with BAPN treatment, associated with a reduction in peak percent area of mature crosslink HP. These findings were made possible by *in vitro* treatment with BAPN and analysis of collagen synthe-

sized entirely under direct inhibition of lysyl oxidase and, thus, enzymatic crosslink formation.

2.7 License and Copyright

The licensed material was modified through: (1) font size increases in the graphs of Fig. 2.3(a) and Fig. 2.3(b); (2) altered formatting in Tables 2.1 and 2.2; (3) modified formatting of text, figure placement and table placement; (4) exclusion of both the Acknowledgments and Author Contributions sections, and (5) migration of the references into the broader reference list associated with the dissertation.

PLOS ONE preferred citation:

Canelón SP, Wallace JM (2016) β-Aminopropionitrile-Induced Reduction in Enzymatic Crosslinking Causes In Vitro Changes in Collagen Morphology and Molecular Composition. PLOS ONE 11(11): e0166392. https://doi.org/10.1371/journal.pone.0166392

3. DOSE-DEPENDENT EFFECTS OF β–AMINOPROPIONITRILE ON OSTEOBLAST PROLIFERATION AND GENE EXPRESSION

3.1 Abstract

Enzymatic crosslinks are responsible for stabilizing the fibrillar structure of type I collagen, and are catalyzed by lysyl oxidase (LOX), a step which can be interrupted using the lathyritic agent β-aminopropionitrile (BAPN). A previous study confirmed the effects of BAPN on *in vitro* collagen nanostructure and crosslink composition at a low BAPN concentration but did not demonstrate a coupled effect on the expression of genes encoding type I collagen or LOX. The objective of this study was to quantify the dose-dependent effect of BAPN on osteoblast gene expression of type I collagen and LOX as well as genes associated with crosslink formation including bone morphogenic protein-1 (*BMP-1*) and periostin (*POST*). The effect on cell proliferation was also evaluated in relation to a broad range of BAPN concentrations.

Osteoblasts were cultured in complete media, and differentiated using ascorbic acid, in the presence or absence of 0.25, 1.0, 2.0, 5.0, or 10.0 mM BAPN for gene expression analysis using quantitative reverse transcription polymerase chain reaction. A second experiment investigated the effect of a broader range of BAPN concentrations (including 0.125 and 0.5mM BAPN) on osteoblast cell proliferation. Results showed significant upregulation of *BMP-1*, *POST*, and *COL1A1* at 1.0, 2.0, and 5mM BAPN and no significant effect of any concentration on the expression of *LOX* or *COL1A2*. We also found that 1.0, 2.0, and 5.0mM produced a significant change in cell proliferation while the lower BAPN concentrations of 0.125, 0.25, and 0.5mM had no effect at the timepoints investigated. The results confirm a dose-dependent osteoblast response to BAPN and show that while the gene encoding LOX remains

unaffected by BAPN treatment, other genes related to LOX activation and matrix production including *BMP-1* and *POST*, are upregulated.

3.2 Introduction

Mature osteoblasts are responsible for synthesizing type I collagen in bone as a right-handed helical structure formed from three polypeptide chains of amino acids. Post-translationally, collagen fibrils are stabilized within their staggered array by intramolecular and intermolecular crosslinks [6, 7, 112]. Enzymatic crosslinks are initiated by the lysyl oxidase (LOX) enzyme and eventually form covalent chemical crosslinks between collagen molecules and fibrils [7, 10, 112]. Crosslink synthesis can be limited by compounds such as penicillamine and β-aminopropionitrile (BAPN), resulting in a crosslink deficiency which characterizes a disease known as lathyrism [113, 114, 143]. BAPN irreversibly binds to the LOX active site preventing LOX from initiating enzymatic crosslinking and thus blocking not only the formation of new crosslinks but also the maturation of pre-existing immature crosslinks.

The ability of LOX to initiate enzymatic crosslinking also depends on direct or indirect interactions with other connective tissue proteins including bone morphogenic protein-1 (BMP-1), periostin (POST), and fibronectin [144–146]. LOX is synthesized as an inactive precursor, pro-LOX, and activated through propeptide proteolytic cleavage carried out by BMP-1. Maruhashi *et al.* found POST binds to BMP-1, enhances proteolytic cleavage of pro-LOX, and promotes the deposition of BMP-1 onto the fibronectin matrix. In addition, their results suggest increased interactions between POST and fibronectin lead to increased enzymatic crosslinking [145]. These relationships are further complicated by interactions with fibronectin which have the potential to impact the structure and function of type I collagen (Fig. 3.1).

While BAPN has been shown to modify nanoscale properties, morphology, and crosslinking of type I collagen produced by osteoblasts *in vitro* [111], knowledge of its direct effects on the osteoblast response is limited [119–121]. The purpose of

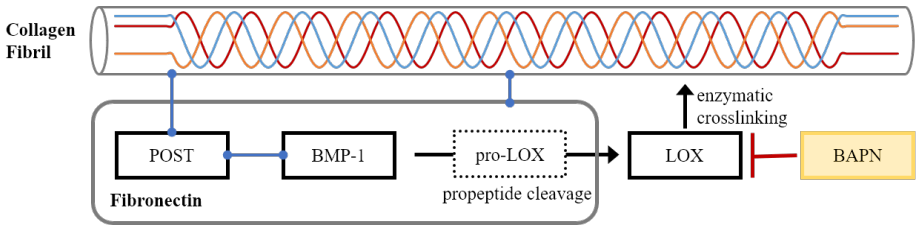

Fig. 3.1. **Complex interactions impacting LOX activation and collagen crosslinking**. LOX activation is dependent on POST and BMP-1 function and its activated form can be irreversibly bound by BAPN, preventing intra- and intermolecular enzymatic crosslink formation. Black boxes and arrows represent the process of LOX activation leading to enzymatic crosslink initiation, blue links represent binding between two components, and the red segment between LOX and BAPN represents the pairs inhibitory effect on crosslinking. POST, BMP-1, and pro-LOX all bind to fibronectin.

this study was to expose osteoblasts to a range of BAPN concentrations to evaluate their temporal proliferation response and the expression of genes related to collagen synthesis and crosslinking. It was hypothesized that (1) LOX and related genes would be upregulated with increasing BAPN dosage to compensate for the reduction in enzymatic crosslinking and (2) osteoblast proliferation would have a dose-dependent negative response to BAPN exposure.

3.3 Material and Methods

3.3.1 Cell culture

MC3T3-E1 Subclone 4 (ATCC^{R} CRL-2593) murine preosteoblasts were obtained from the American Type Culture Collection (ATCC, Manassas, VA) and cultured in proliferation medium composed of α minimal essential medium (α-MEM, Life Technologies, Carlsbad, CA), 10% fetal bovine serum (FBS, GIBCO, Carlsbad, CA), 0.5% penicillin/streptomycin (GIBCO, Carlsbad, CA), and 1% L-glutamine (Hyclone, Logan, UT). MC3T3-E1 differentiation control medium consisted of prolif-

eration medium supplemented with 50μg/ml ascorbic acid (Thermo Fisher Scientific,Waltham, MA) and differentiation experimental medium was additionally supplemented with 0.125, 0.25, 0.5, 1, 2, 5, or 10mM BAPN (Sigma Aldrich, St. Louis, MO) for crosslink inhibition experiments. The cells were cultured in T75 flasks and allowed to proliferate until reaching 80% confluence. Once confluent, the cells were seeded into 6-well plates for the qRT-PCR assay and 96-well plates for the cell proliferation assay. After seeding, the medium was replaced and supplemented with ascorbic acid to allow for differentiation and to promote collagen synthesis. BAPN-treated wells were additionally supplemented with one of seven BAPN dosages while those left untreated served as control wells.

3.3.2 Quantitative reverse transcription polymerase chain reaction (qRT-PCR)

Cells from a single flask were seeded into eight 6-well plates (500,000 cells per well), one of them a control plate without BAPN and the remaining seven each treated with a different BAPN dosage (n=5 per group). At the end of a 7 day differentiation period, the medium was removed from each culture dish and replaced with 1mL of TRIzol reagent (Invitrogen, CA). RNA isolation was performed using TRIzol reagent and reverse transcription (RT) was carried out using a High Capacity cDNA Reverse Transcription Kit (Life Technologies, Carlsbad, CA). PCR was performed using an ABI 7500 Fast PCR machine with SYBR Green primers using the Standard cycling mode modified for the PowerUp SYBR Green PCR master mix (Life Technologies, Carlsbad, CA). Primers were chosen for target genes encoding type I collagen α1 (*COL1A1*), type I collagen α2 (*COL1A2*), *LOX*, *BMP-1*, *POST*, as well as reference gene 18s RNA (*18S*) (Table 3.1) [125].

Each sample/gene combination was run in triplicate and water was used as the no-template control. mRNA expression levels of the triplicates were averaged. Following an efficiency-calibrated mathematical model [126], mRNA expression levels

Table 3.1.

Primer sequences (5' to 3') used for qRT-PCR.

Target Gene	**Forward**	**Reverse**
COL1A1	GCAACAGTCGCTTCACCTACA	CAATGTCCAAGGGAGCCACAT
COL1A2	CAGAACATCACCTACCACTGCAA	TTCAACATCGTTGGAACCCTG
LOX	TACTCCAGACTCTGTGCGCT	GGACTCAGATCCCACGAAGG
BMP-1	CTTCCCTCAATCACCCAGACT	TAAAGATTAGGGACACCGGCTA
POST	GGAATTCGGCATTGTGGGAGCCACTACC	GGTCGACTCAAATTTGTGTCAGGACACGGTC
18S	GTAACCCGTTGAACCCCATT	CCATCCAATCGGTAGTAGCG

for each sample/target gene were averaged and compared to the control group using the REST [R] program [127]. The program calculates relative expression ratios using Equation 3.1 and employs randomization tests to obtain a level of significance.

$$Ratio = \frac{(E_{Target})^{\Delta CT_{Target}(Control-Sample)}}{(E_{Ref})^{\Delta CT_{Ref}(Control-Sample)}} \tag{3.1}$$

E_{Target} and E_{Ref} are the qRT-PCR efficiencies of a target gene and reference gene transcript, respectively; and ΔCT is the difference in control and sample cycle thresholds for the respective gene transcript.

3.3.3 Cell proliferation assay

Cells from a single flask were seeded into three 96-well plates (5,000 cells per well), corresponding to BAPN treatment periods of 24, 48, and 72 hours. Within each plate, cells were seeded into 8 columns, one of them with control wells and the remaining seven each treated with a different BAPN dosage (n=5 per group). The CellTiter 96 [R] AQ_{ueous} One Solution Cell Proliferation Assay (Promega, Madison, WI) was used as a colorimetric method to determine the number of viable cells after BAPN treatment periods of 24, 48, or 72 hours. At the end of each treatment period, 20μL of CellTiter 96 [R] AQ_{ueous} One Solution Reagent was added to each well according to manufacturer instructions and the plate was incubated for 2 hours. The absorbance was then read at 490nm using an ELx800 microplate reader (BioTek, Winooski, VT) to measure the soluble formazan produced from the cellular reduction of the reagents tetrazolium compound, a measurement directly proportional to the number of living cells in culture.

3.3.4 Statistical analysis

Differences in mRNA expression between control and BAPN-treated samples were assessed using the REST [R] program in group means for statistical significance by using a Pair Wise Fixed Allocation Random Test [c].

The cell proliferation absorbances were tested for a main effect of BAPN dosage using a one-way ANOVA for each time point followed by Dunnett's multiple comparisons test using GraphPad Prism version 7.04 for Windows (GraphPad Software, La Jolla, CA).

A value of $p<0.05$ was considered significant for all experiments.

3.4 Results

3.4.1 qRT-PCR of cellular gene expression

Significant upregulation of *BMP-1*, *POST*, *COL1A1*, *COL1A2* was observed with exposure to various BAPN concentrations. Significant upregulation was noted at all concentrations for *BMP-1*, concentrations greater than 0.25mM for *POST*, and 1.0mM, 2.0mM, and 10.0mM BAPN for *COL1A1* and *COL1A2* (Table 4.2). *LOX* was upregulated at 1.0, 5.0, and 10.0mM though not to a statistically significant degree.

Table 3.2.
Fold changes in mRNA expression of BAPN-treated samples relative to controls (n=3 for LOX, n=5 for all other targets). *Indicates statistically significant changes ($p<0.05$).

Target Gene	**0.25mM**	**1.0mM**	**2.0mM**	**5.0mM**	**10mM**
LOX	0.737	1.138	0.934	1.402	1.469
BMP-1	2.072*	2.705*	2.622*	2.212*	2.299*
POST	1.207	3.443*	4.407*	6.058*	10.468*
COL1A1	1.327	1.835*	2.179*	1.724	1.897*
COL1A2	1.517	1.652*	1.944*	1.395	1.892*

3.4.2 Cell proliferation assay

The cell proliferation results showed a trend of increased proliferation with increasing BAPN concentration at all three time points followed by a decline in proliferation at 10.0mM after 48 and 72 hours. The decline in proliferation was more pronounced at the 48 and 72 hour time points (Fig. 3.2).

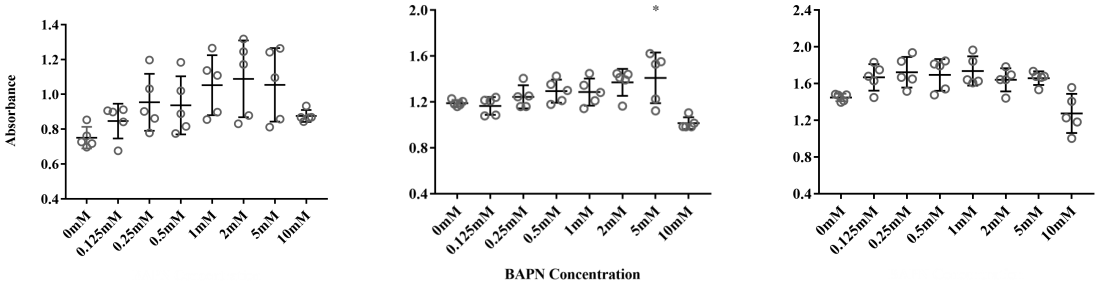

(a) 24 Hours (b) 48 Hours (c) 72 Hours

Fig. 3.2. **Cell proliferation as a function of BAPN dosage (n=5)**. Proliferation after (a) 24 hours, (b) 48 hours, and (c) 72 hours. Statistically significant changes relative to 0mM BAPN controls indicated by * ($p<0.05$) and ** ($p<0.01$).

After 24 hours of exposure to BAPN, a significant increase in proliferation relative to the 0mM BAPN control was found for 1mM ($p=0.0240$), 2mM ($p=0.0095$), and 5mM ($p=0.0231$) concentrations, while the cellular response at all other BAPN concentrations was not significantly different. The same was true for 5.0mM BAPN ($p=0.0276$) at the 48 hour time point, and for 0.25mM ($p=0.0315$) and 1.0mM ($p=0.0218$) at the 72 hour time point (Table 3.3).

Table 3.3.
Significant mean differences in absorbance relative to 0mM BAPN controls (n=5). Statistically significant changes indicated by * ($p<0.05$) and ** ($p<0.01$)

Concentration (mM)	24 Hours	48 Hours	72 Hours
0.125	0.0954	-0.0246	0.2194
0.25	0.2028	0.0546	0.2742*
0.5	0.1852	0.1042	0.2454
1.0	0.3012*	0.0962	0.2884*
2.0	0.3374**	0.1808	0.1926
5.0	0.3028*	0.2200*	0.2098
10.0	0.1246	-0.1750	-0.1740

3.5 Discussion

It was hypothesized that *LOX* and related genes would be upregulated with increasing BAPN dosage to compensate for the reduction in enzymatic crosslinking. The results indicated this was true for multiple genes across many BAPN concentrations. *BMP-1*, *POST*, *COL1A1* and *COL1A2* were upregulated at most dosage levels greater than 0.25mM. In particular, *POST* expression increased in a dose-dependent manner. *LOX* was unaffected even at 10.0mM BAPN which was roughly 70x higher than the concentration used in prior *in vitro* studies showing changes in collagen morphology and crosslinking [111]. This confirmed the idea that factors other than expression of *LOX* were regulating the structural changes in response to BAPN. Superficially it would appear that BAPN upregulation of *POST* could have influenced the upregulation of *BMP-1*, as part of the LOX activation process, however Maruhashi *et al.* revealed no significant difference in *BMP-1* expression between wild type (WT) and periostin $^{-/-}$ calvarial osteoblasts [145]. This supports the idea that exposure to

BAPN rather than specifically the upregulation of *POST* was the driving force for *BMP-1* regulation in the present study.

The structural and biochemical changes reported by Canelón and Wallace [111] may have originated from a difference in extracellular availability of activated LOX versus the pro-LOX precursor. Low levels of BAPN in the present study resulted in significant upregulation of *BMP-1* at 0.25mM BAPN relative to the control suggesting a compensatory effect to increase BMP-1-mediated processing of pro-LOX in response to BAPN exposure. This effect is further supported by the significant upregulation of genes encoding type I collagen, *COL1A1* and *COL1A2*, in the presence of BAPN. The low BAPN concentration in this study was roughly twice that of the concentration used in Canelón and Wallace, so it is unclear whether the changes in collagen morphology and crosslinking occurred regardless of any compensatory mechanism.

The second hypothesis of this study predicted osteoblast proliferation would have a dose-dependent negative response to BAPN exposure. We observed the opposite effect with proliferation increasing with BAPN concentration and declining at the highest concentration of 10.0mM, particularly after 48 and 72 hours. In addition to the BAPN concentrations included in the gene expression analysis, 0.125mM and 0.5mM were also investigated for their effects on cell proliferation. MC3T3-E1 cells are known to actively replicate during the initial development phase between 1 and 9 days of culture [147]. Observation of the BAPN effect on cell proliferation was limited to a culture period of three days at the end of which proliferation trended downward, particularly at the highest concentration. This suggests a temporary effect possibly caused by BAPN-mediated upregulation of early osteogenic genes not considered in this study, and the potential for a greater decline in proliferation over a longer exposure period. The absence of a negative impact of BAPN on cell proliferation further supports the more complex mechanism-driven theory alluded to above in the discussion of mRNA expression responses to BAPN treatment.

The gene expression findings coupled with the cell proliferation data encourage exploration of how these effects translate to type I collagen protein properties at concentrations higher than those previously investigated [111]. The gene expression data would suggest 1.0, 2.0, or 10.0mM BAPN for the significant upregulation of collagen-related genes, namely *COL1A1*, *COL1A2*, *BMP-1*, and *POST*. Cell proliferation data would caution against exposure to 10.0mM BAPN for risk of a continued decrease in cellular metabolic activity with longer culture periods required for type I collagen accumulation. For these reasons, characterization of type I collagen produced *in vitro* with exposure to 1.0mM or 2.0mM BAPN would be advantageous in future studies. Future protein level expression studies would also help elucidate the correlation between the mRNA expression response found in this study and translation outcomes.

3.6 Conclusions

In conclusion, genes encoding type I collagen and enzymatic crosslinking steps were upregulated with exposure to BAPN suggesting a mechanism of compensation in response to the reduction in active LOX available to initiate enzymatic crosslinking. The unpredicted positive influence of BAPN dosage on cell proliferation early in the osteoblast differentiation process highlighted the need for more thorough study of influences on osteogenic markers in the presence of the BAPN compound and its complex interactions with LOX, BMP-1, and POST.

4. EFFECTS OF SUBSTRATE STRAIN ON TYPE I COLLAGEN PROPERTIES AND CROSSLINKING IN THE PRESENCE OF β–AMINOPROPIONITRILE

4.1 Abstract

Enzymatic crosslinking stabilizes the fibrillar structure of type I collagen and can be interrupted by irreversible binding of the lysyl oxidase (LOX) enzyme by the lathyritic agent beta-aminopropionitrile (BAPN). Results from the dose-dependent study described in chapter 4 demonstrated a dose-dependent effect on genes encoding type I collagen, *COL1A1* and *COL1A2*, and those involved in collagen crosslinking including *LOX*, bone morphogenetic protein-1 (*BMP-1*), and periostin (*POST*). Mechanical loading is known to impact osteoblast behavior and even compensate for changes in type I collagen morphology resulting from BAPN-mediated enzymatic crosslinking inhibition [137]. The objective of the present investigation was to characterize the collagen produced *in vitro* after MC3T3-E1 exposure to 2.0mM BAPN and explore changes to its properties under continuous cyclical loading using applied substrate strain. The impact of mineralization was also evaluated for its influence on mature and immature enzymatic crosslinking.

Osteoblasts were cultured in complete media and differentiated using ascorbic acid 2-phosphate in the presence or absence of 2.0mM BAPN. Cells used in crosslinking experiments were further differentiated using mineralization media containing 10mM β-glycerophosphate. The study design included four groups to compare the effects of BAPN treatment and mechanical loading: (1) control-static, (2) control-load, (3) BAPN-static, (4) BAPN-load. Atomic force microscopy (AFM) was used to execute AFM-based nanoindentation to extract elastic properties of the collagen matrix, Fourier Transform infrared spectroscopy was used to assess collagen secondary

structure for enzymatic crosslinking analysis, and quantitative reverse transcription polymerase chain reaction was used to quantify mRNA expression. Results showed a higher indentation modulus in samples treated with BAPN and loaded compared to control samples under load. Mechanical loading increased the 1660cm^{-1} to 1690cm^{-1} peak area ratio (mature and immature crosslinks, respectively) and peak height ratio in control samples, and BAPN treatment increased the height ratio in static samples. BAPN upregulated *BMP-1* in static samples and BAPN combined with mechanical loading downregulated *LOX* when compared to control-static samples.

4.2 Introduction

As a composite material, bone is made up of an inorganic hydroxyapatite mineral phase, a proteinaceous organic phase, and water. Type I collagen is the most abundant protein in the human body [102] and makes up 90% of the organic phase. Hydroxyapatite and collagen both contribute to bone mechanical properties: hydroxyapatite provides compressive strength and stiffness while collagen provides tensile strength and ductility [22,103,104]. Property changes in either phase can impact bulk mechanical properties of the tissue and bone structure and can compromise structural and functional integrity.

Mature osteoblasts are responsible for synthesizing type I collagen in bone as a right-handed helical structure formed from three polypeptide chains of amino acids. Each chain is a left-handed helix with repeating Gly-X-Y triplets where Gly is glycine, X is usually proline, and Y hydroxyproline [5,110]. Two of these polypeptide chains are $\alpha 1$ helices and one is an $\alpha 2$ helix forming a triple-helix type I collagen molecule. Once formed, N and C terminal ends are cleaved by proteinases, leaving mature collagen molecules. These molecules self-assemble in-line into microfibrils, then in parallel into arrays, and finally into three-dimensional fibrils.

Collagen fibrils are stabilized within their staggered array by intramolecular and intermolecular crosslinks [6, 7, 112]. Enzymatic crosslink formation is initiated by

lysyl oxidase (LOX) when telopeptide precursors convert to telopeptide aldehydes which in combination with other precursors form covalent chemical crosslinks [7, 10]. Some of these crosslinks mature to their trivalent form as pyridinolines (i.e. HP, hydroxypyridinoline) and pyrroles. Compounds like β-aminopropionitrile (BAPN) limit crosslink formation by irreversibly binding to the LOX active site and preventing LOX from catalyzing aldehyde formation necessary to form new crosslinks and mature pre-existing immature ones.

In addition to synthesizing collagen, osteoblasts also interact with osteoclasts and osteocytes to carry out bone modeling and remodeling processes in response to their mechanical environment [59]. Because of this role in bone development, it is important to examine the osteoblast response to mechanical loading, and its effects on structural, biochemical, and mechanical properties of the secreted collagen matrix. Exercise has been found to have positive effects on bone structure and strength [148, 149] and mechanical loading of diseased bone has been shown to have compensatory effects on collagen properties [116, 137]. The effects of mechanical loading on the properties of collagen produced *in vitro* by osteoblasts have yet to be explored, much less characterized.

BAPN has been shown to modify nanoscale properties, morphology, and crosslinking of type I collagen produced by osteoblasts *in vitro* [111], but has not been evaluated for its effect on collagen mechanical properties nor has mechanical loading been explored for its potential compensatory effect on diseased collagen. It was hypothesized that BAPN-mediated inhibition of collagen crosslinking would (1) alter the elastic properties of type I collagen, (2) inhibit the formation of mature enzymatic crosslinks, and (3) upregulate *BMP-1*, *POST*, *COL1A1*, and *COL1A2*. Mechanical loading was hypothesized to influence properties impacted by BAPN treatment.

4.3 Materials and Methods

4.3.1 Cell culture

MC3T3-E1 Subclone 4 (ATCC® CRL-2593) murine preosteoblasts were obtained from the American Type Culture Collection (ATCC, Manassas, VA) and cultured in proliferation medium composed of α minimal essential medium (α-MEM) (Life Technologies, Carlsbad, CA), 10% fetal bovine serum (FBS) (GIBCO, Carlsbad, CA), 0.5% penicillin/streptomycin (GIBCO, Carlsbad, CA), and 1% L-glutamine (Hyclone, Logan, UT). MC3T3-E1 differentiation control medium consisted of proliferation medium supplemented with 50μg/ml ascorbic acid 2-phosphate (Sigma Aldrich, St. Louis, MO) and differentiation experimental medium was additionally supplemented with 2.0mM BAPN (Sigma Aldrich, St. Louis, MO) for crosslink inhibition experiments. For collagen crosslinking analysis, mineralization medium was made by supplementing both the control and BAPN differentiation media with 10mM β-glycerophosphate (EMD Millipore, Danvers,MA).

The cells were cultured in T75 flasks and allowed to proliferate until reaching 80% confluence. Once confluent, the cells were seeded into 6-well plates with flexible silicone bottoms coated with fibronectin to enhance adhesion for all of the experiments presented here. After seeding, the medium was replaced and supplemented with ascorbic acid to allow for differentiation and to promote collagen synthesis. A total of four groups were considered for this study to investigate the effects of BAPN treatment and mechanical loading: control-static, control-load, BAPN-static, BAPN-load.

4.3.2 Mechanical loading

All cells were cultured in BioFlex® ProNectin 6-well culture plates coated with fibronectin and specially designed to respond to cyclic substrate strain *in vitro* applied by a Flexcell® FX-4000 computer-regulated vacuum pressure strain unit (Flexcell®

International Corp., Burlington, NC). The unit applied a defined and controlled mechanical strain to samples in the control-load and BAPN-load groups by using sinusoidal negative vacuum pressure to deform the cell substrate. Control-static and BAPN-static samples were simultaneously cultured in the same incubator and adjacent to the strain unit during the loading period.

Cells were cyclically loaded to 5% elongation at 3 cycles/min (10 seconds strain, 10 seconds relaxation; 0.2Hz frequency) continuously for 7 days with a pause at day 3 to change media. It is worth noting that a circular loading post (25mm in diameter) was used to apply tension to the cell culture well which has been shown to result in biaxial strain across the surface directly over the post and a relatively large radial strain in the region in contact with the outer edge of the post [150]. One 7 day loading experiment was run per assay for this investigation and the manufacturer-recommended drying regimen was run between each 7 day loading period.

4.3.3 Quantitative reverse transcription polymerase chain reaction (qRT-PCR)

Cells were seeded into four 6-well Bioflex plates (100,000 cells per well) and cultured in differentiation media with or without BAPN. At the end of a 7 day loading period, the media was removed from each well and replaced with 1mL of TRIzol reagent (Invitrogen, CA). RNA isolation was performed using TRIzol reagent and reverse transcription (RT) was carried out using a High Capacity cDNA Reverse Transcription Kit (Life Technologies, Carlsbad, CA). An ABI 7500 Fast PCR machine was used to perform PCR with SYBR Green primers and under the Standard thermal cycling mode modified for PowerUp SYBR Green PCR master mix (Life Technologies, Carlsbad, CA). Primers were chosen for target genes encoding type I collagen α1 (*COL1A1*), type I collagen α2 (*COL1A2*), *LOX*, *BMP-1*, *POST*, as well as reference gene 18s RNA (*18S*).

Each sample/gene combination was run in triplicate and RNAse-free water was used as the no-template control. mRNA expression levels of the triplicates were averaged. Following an efficiency-calibrated mathematical model [126], mRNA expression levels for each sample/target gene were averaged and compared to the control group using the REST ^{R} program [127].

4.3.4 Fourier transform infrared (FTIR) spectroscopy

Using the same experimental methods described above, another set of experiments was performed to analyze the secondary structure of type I collagen using FTIR. Cells were seeded into four 6-well BioFlex plates (one per experimental group) at a density of 80,000 cells per well and cultured in mineralization media with or without BAPN. Following 7 days of mechanical loading, the plates were cultured for another 21 days under static conditions to allow time for collagen deposition and mineralization. In preparation for FTIR data collection, media was removed and plates were rinsed four times with sterile milli-Q water. Samples were left hydrated overnight for the matrix to lift off of the substrate. Matrix samples were carefully transferred from their wells to barium fluoride windows using a cell scraper and rubber-coated tweezers, and air-dried.

FTIR spectroscopic analysis was performed using a Nicolet iN 10 infrared microscope (Thermo Fisher Scientific, Waltham, MA). A water vapor background was collected and subtracted from sample data as they were acquired. Data were collected from the samples at room temperature at a spectral resolution of 4cm^{-1}. The amide I and amide II regions ($\sim$1400-1800cm^{-1}) were baseline corrected according to published standards [128,129] using OriginPro 2018 (OriginLab, Northampton, MA). Second derivative analysis was used to resolve underlying peaks within these regions and each spectrum was curvefit with Gaussian peaks using GRAMS/AI (Thermo Fisher Scientific, Waltham, MA). The results from the converged peak fitting were expressed as peak position, percentage area of the peak relative to the area underneath

the fitted curve, and peak height. This investigation focused on peaks corresponding to positions at $\sim$1660cm^{-1} and $\sim$1690cm^{-1}, shown to be correlated to mature (HP, hydroxylysylpyridinoline) and immature crosslinks, respectively [120, 121, 130, 131].

4.3.5 Atomic force microscopy (AFM)-based indentation

In order to analyze elasticity of the type I collagen matrix, cells were seeded in four 6-well BioFlex plates (one per experimental group) as described in the FTIR methods above. The loaded groups were loaded as described above for a period of 7 days. The cells were then cultured for an additional 7 days under static conditions and in proliferation medium prior to data collection. Prior to indentation, one well/sample per group was prepared through rinsing three times with phosphate-buffered saline (PBS). At this point the PBS was aspirated and the well's silicone membrane was cut out using a disposable scalpel blade and carefully transferred to a 60mm dish. About 3mL of PBS was then added to the 60mm dish in order to maintain sample hydration during indentation. After one sample from each group was indented, another set of samples was prepared.

Multiple locations within each dish were indented in fluid and at room temperature ($\sim$24^{o}C) with a Bioscope Catalyst AFM (Bruker, Santa Barbara, CA) in contact mode using a single calibrated bead AFM probe (Novascan Technologies, Boone, IA). This gold-coated silicon nitride probe had an attached borosilicate glass bead (5μm in diameter and spring constant of 0.065N/m). Before indenting, the probe was pushed onto a glass surface and the cantilever deflection was used to measure the probes deflection sensitivity (nm/V). The AFM is mounted on a Leica DMI3000 inverted microscope (Leica Biosystems Inc., Buffalo Grove, IL) which allowed collagenous areas of interest to be identified. Indentations were made to a trigger force of 1nN at a speed of 0.5Hz and force-separation curves were acquired. On average, 7-10 areas were indented per sample for a total of 22-39 indents per group. A linear baseline correction was applied to the retraction curve and the reduced elastic modulus was

fit for each unloading curve for roughly 15% to 70% of the maximum force using the Hertz model of elastic contact as reported by our group elsewhere [43].

4.3.6 Statistical analysis

Anderson-Darling tests were used to detect indentation modulus distribution differences between each group.

The amide I peak area ratios, peak height ratios, and peak heights were tested for main effects of BAPN treatment and mechanical loading using a two-way ANOVA followed by a Tukey multiple comparisons test using GraphPad Prism version 7.04 for Windows (GraphPad Software, La Jolla, CA).

Differences in mRNA expression between control-static samples and each of the other three groups (control-load, BAPN-static, BAPN-load) using the REST [R] program in group means for statistical significance by using a Pair Wise Fixed Allocation Random Test [c] .

A value of $p<0.05$ was considered significant for all experiments.

4.4 Results

4.4.1 qRT-PCR of cellular gene expression

All mRNA expression data was analyzed with respect to the control-static group. *LOX* was significantly downregulated in the BAPN-load group with respect to the control-static group ($p=0.019$). *BMP-1* was seen to significantly increase with BAPN treatment when comparing BAPN-static and control-static groups ($p=0.029$)(Table 5.1).

Table 4.1.
Fold changes in mRNA expression in all samples relative to the control-static group (n=4). *Indicates statistically significant changes ($p<0.05$).

Target Gene	Control-Load	BAPN-Static	BAPN-Load
LOX	0.743	0.707	0.593*
BMP-1	1.17	1.334*	1.264
POST	1.639	1.15	1.272
COL1A1	1.162	1.052	0.978
COL1A2	1.1	1	1.075

4.4.2 Amide I crosslinking from FTIR spectra

Areas of interest for crosslinking analysis were identified using the infrared microscope and data acquired from a minimum of five locations per sample. These five spectra were fit for underlying peaks and the results averaged to equal an n of 1. Spectra were collected from as many samples as possible though challenges arose during sample preparation and some samples became suboptimal for data collection. This resulted in sample size variation among groups: control-static, n=6; control-load, n=4; BAPN-static, n=6; BAPN-load, n=5. Peak fitting in the amide I region resulted in consistent peaks around 1688cm^{-1} and 1661cm^{-1} and were considered to be representative of HP and immature crosslinks, respectively.

Statistical analysis found a significant interaction between treatment and loading ($p=0.0244$) for the 1660:1690 peak area ratio (data not shown). Post-hoc analysis showed a significant increase in control-load versus control-static samples ($p=0.0188$). An interaction was also found for the 1660cm^{-1} peak area ($p=0.0014$) and post-hoc analysis found a significant increase in control-load relative to control-static samples ($p=0.0132$), and a decrease in BAPN-load compared to control-load samples ($p=0.0163$). In analyzing the ratio between amide I peak heights, a significant in-

teraction (p=0.0006) was also detected. Post-hoc analyses indicated a significant increase when comparing control-static samples to both control-load (p=0.0135) and BAPN-static (p=0.0012) samples (Fig. 4.1).

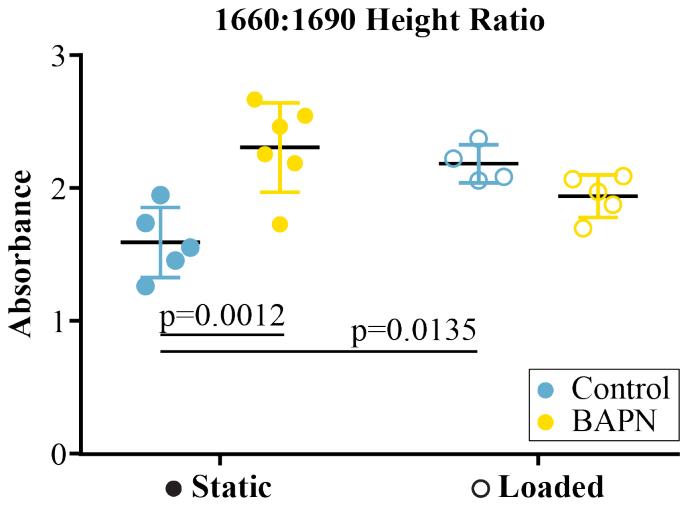

Fig. 4.1. **Scatter plot of height ratio data (mean ± standard deviation)**. An increase in the ratio of 1660cm^{-1} to 1690cm^{-1} peak height is evident in control-static and BAPN-load relative to control-static. Significant differences are indicated by black bars between groups accompanied by p-values.

While a treatment-load interaction was discovered during analysis of the 1660cm^{-1} and 1690cm^{-1} peak heights (p=0.0074), the post-hoc test did not reveal any significant differences in peak height comparisons across groups. However, there was a trend towards an increased 1660cm^{-1} peak height in the control-load group compared to the control-static group (p=0.0827).

4.4.3 Elastic modulus from AFM indentation

Indentation was performed in each sample at as many locations as possible but identifying areas and acquiring indentation data from BAPN samples proved more challenging than with control groups. This was likely due to a difference in adhesion

due to the presence of BAPN, and led to differences in sample size and number of indents: control-static, n=5; control-load, n=4; BAPN-static, n=4; BAPN-load, n=3. The BAPN-static group was found to have the highest mean indentation modulus at 0.251 ± 0.031kPa and caused a significant increase relative to control-static samples at 0.239 ± 0.032kPa (p=0.0499) (Fig. 4.2). Mechanically loaded control samples had a mean modulus value of 0.216 ± 0.025kPa, which trended downward relative to static control samples (p=0.0882) (Fig. 4.3). There was no discernible difference between control-static and BAPN-load groups (0.231 ± 0.011kPa).

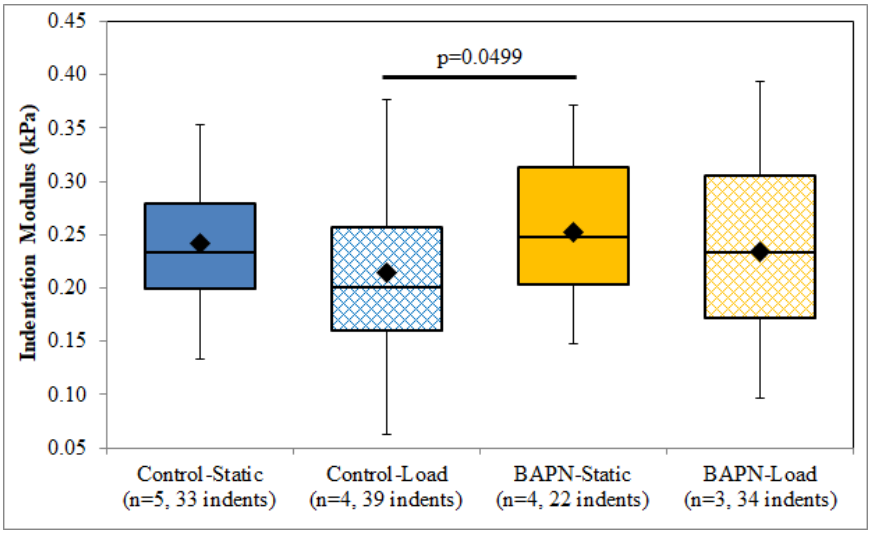

Fig. 4.2. **Boxplot representation of the spread of indentation modulus data**. An increase in mean indentation modulus is evident in the BAPN-static samples relative to control-load samples, as is the similarity between the control-static and BAPN-load groups. Mean values are marked by the diamond marks on the boxplots.

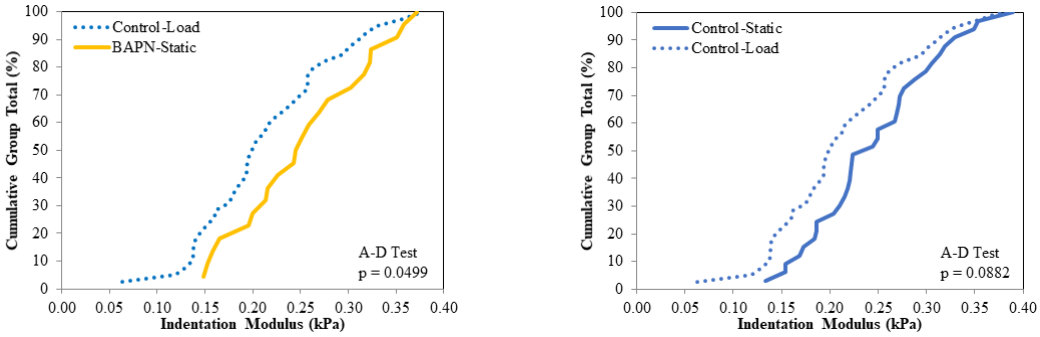

(a) Control-Load vs. BAPN-Static

(b) Control-Load vs. Control-Static

Fig. 4.3. **Cumulative distribution function representation of indentation modulus data**. There is a clear shift towards a (a) higher indentation modulus in the BAPN-static group relative to the control-load group and (b) lower indentation modulus in the control-load group relative to control-static.

4.5 Discussion

It was hypothesized that BAPN would upregulate *BMP-1*, *POST*, *COL1A1*, and *COL1A2* in accordance with results from the dose-dependent BAPN study described in chapter 4. This trend was consistent in this study when comparing the BAPN-static group to the control-static group; however, upregulation of *BMP-1* was the only significant outcome. This upregulation of *BMP-1* in the presence of BAPN supports a compensatory mechanism to increase the conversion of the LOX precursor to its active form capable of initiating enzymatic crosslinking. Mechanical loading was also found to upregulate *BMP-1* in both control and BAPN groups, though not significantly. However, loading did appear to mitigate the effect of BAPN on *BMP-1* expression, as evidenced by the lack of an effect in the BAPN-load group. The effect of loading was also clearly seen in the significant downregulation of *LOX* with BAPN treatment relative to static controls, as it caused more pronounced downregulation than its BAPN-static counterpart. In addition, loading alone did not produce an effect on the gene regulation as evidenced by no differences in mRNA expres-

sion between control-load and control-static samples. This decrease in *LOX*, under loaded conditions, suggests that the strain experienced by the osteoblasts negatively impacted the availability of the LOX precursor, thereby limiting the availability of activated LOX and potential for enzymatic crosslinking.

Second derivative analysis of the type I collagen FTIR spectra revealed underlying peaks corresponding to HP and immature crosslinks. Part of our hypothesis stated that BAPN would inhibit the formation of mature enzymatic crosslinks. Treatment with BAPN increased the mature/immature peak height ratio in static samples and caused a decline in HP peak area in loaded samples. This BAPN-mediated decrease in mature crosslinking was consistent with a past study [111] although in loaded rather than static conditions. Taking both of these cases together, BAPN inhibition of enzymatic crosslinking via LOX inhibition was confirmed by the decrease in the peak area corresponding to mature crosslink HP, regardless of mechanical loading. When considering the effect of loading on collagen crosslinking, loading was found to increase the mature/immature peak area ratio in control samples, a change driven by a significant increase in the HP peak area. It also was shown to mitigate the effects seen with BAPN-control samples. Under normal circumstances (absent BAPN LOX inhibition), mechanical loading has a positive influence on enzymatic crosslinking verified through increases in the HP peak area, mature/immature area ratio, and mitigative effects on BAPN inhibition.

Our hypothesis also stated that BAPN-mediated inhibition of collagen crosslinking would impact the elastic properties of type I collagen. An upward trend in modulus for BAPN samples compared to controls led to a significant increase in modulus in BAPN-static conditions relative to control-load conditions. Because of the interaction between both BAPN and loading, interpretation of the influence of either effect would benefit from further exploration. However, we can conclude that BAPN did not have a similar significant effect relative to the Control-Load under Loaded conditions which points to loading having a mitigative effect on BAPN-mediated changes to elastic modulus. While BAPN did not have a clear broad effect on collagen elasticity,

it impacted enzymatic crosslinking as noted above, suggesting that crosslinking along the length of the collagen fibril may not be as influential to the elastic modulus as measured here using AFM-based indentation. This possibility could be explored in future studies by using alternative and perhaps creative methods. One might involve modifying the Flexcell loading regimen to hold a defined well pressure for a determined period of time and calculate the substrate strain applied at that pressure. The indentation data showed a downward trend in modulus for loaded samples compared to static samples suggesting the cyclic strain applied to the cell substrate began to hinder formation of a stabilized collagen matrix. While the change was not significant, the proposed mechanism is substantiated by the observed decrease in LOX described above. Future experiments might consider a decreased applied substrate stretch, modified loading frequency, or decreased loading period.

4.6 Conclusion

In conclusion, BAPN-mediated lysyl oxidase inhibition impacted mRNA expression of *BMP-1* and *LOX*, influenced mature collagen crosslinking under static conditions, and had an interactive effect with loading on indentation modulus. Changes to the *BMP-1* expression appeared compensatory in nature and likely impacted the activated lysyl oxidase available to initiate enzymatic crosslinking. Mechanical loading increased mature/immature peak area ratios and BAPN increased mature/immature peak height ratios in static controls. Finally, an interaction between loading and BAPN treatment influenced collagen elasticity warranting further investigation. In each characterization, mechanical loading was found to have a mitigative effect on BAPN-mediated inhibition.

5. SUMMARY

This dissertation has highlighted the importance in understanding changes to the type I collagen matrix as a result of disease or in response to mechanical loading as it performs multiple functions critical to the musculoskeletal system while manifesting complex properties that transcend levels of bone hierarchy. *In vitro* osteoblast cultures were exposed to the β-aminopropionitrile (BAPN) compound introduced in order to prompt a reduction in enzymatic crosslinking of the synthesized type I collagen matrix. This reduction results from irreversible binding of BAPN to the lysyl oxidase enzyme responsible for catalyzing enzymatic crosslink formation. Alteration of this post-translational modification step was studied for its effect on structural, biochemical, and mechanical properties. In addition, this dissertation evaluates the potential for mechanical loading, via substrate strain, to influence properties affected by reduced enzymatic crosslinking.

Type I collagen was synthesized in the **Chapter 2** study under osteoblast exposure to a low concentration of BAPN. This concentration was found to affect type I collagen morphology as well as secondary structure. Reduced enzymatic crosslinking led to an increase in collagen D-spacing and decrease in the proportion of mature to immature crosslinks. These changes occurred despite no response in expression of genes related to type I collagen synthesis, which prompted the investigation described in chapter 3.

Chapter 3 evaluated the potential for a dose-dependent response to BAPN, assessed by gene expression quantification and a cell proliferation assay. Osteoblast proliferation over a three day period increased as BAPN concentration increased, and multiple genes involved in lysyl oxidase activation and collagen synthesis were upregulated in the presence of high BAPN concentrations. These results encouraged

further characterization of collagen at a high BAPN concentration as described in chapter 4.

Along with further characterization of osteoblast-synthesized collagen, **chapter 4** also aimed to introduce mechanical loading via substrate strain to explore its potential for altering the effects seen by the BAPN-mediated inhibition of enzymatic crosslinking. The higher BAPN concentration used for this investigation caused a decrease in the ratio of mature to immature crosslinking in static samples much like the low concentration did in the chapter 2 study. Mechanical loading was found to increase this ratio in the absence of BAPN. Finally, the lysyl oxidase gene was downregulated while the gene encoding its activator, bone morphogenetic protein-1, was upregulated in response to BAPN. BAPN-mediated enzymatic crosslink reduction and mechanical loading were found to have an interactive effect on elastic modulus of the collagen matrix which motivates future studies. Mechanical loading was found to lessen the extent of any BAPN-mediated changes to enzymatic crosslinking, bone morphonenetic protein-1 expression, and collagen elasticity.

While the work in this dissertation contributed to addressing the gap of knowledge surrounding the translation of type I collagen properties through bone hierarchy, much remains to be explored. The purpose of continuing this work with the intent to connect basic research to a clinically relevant application would be to highlight opportunities for bone disease diagnoses before tissue-level function is compromised.

REFERENCES

REFERENCES

[1] P. Charles, L. Mosekilde, L. Risteli, J. Risteli, and E. Fink Eriksen, "Assessment of bone remodeling using biochemical indicators of type I collagen synthesis and degradation: relation to calcium kinetics," *Bone and Mineral*, vol. 24, no. 2, pp. 81–94, 1994.

[2] R. H. Christenson, "Biochemical markers of bone metabolism: an overview." *Clinical biochemistry*, vol. 30, no. 8, pp. 573–93, 12 1997.

[3] R. Wenstrup, A. Shrago-Howe, L. Lever, C. L. Phillips, P. Byers, and D. Cohn, "The effects of different cysteine for glycine substitutions within alpha 2(I) chains," *Journal of Biological Chemistry*, vol. 266, no. 4, pp. 2590–2594, 2 1991.

[4] L. Risteli and J. Risteli, "Biochemical Markers of Bone Metabolism," *Annals of Medicine*, vol. 25, pp. 385–393, 1993.

[5] V. Ottani, D. Martini, M. Franchi, A. Ruggeri, and M. Raspanti, "Hierarchical structures in fibrillar collagens," *Micron*, vol. 33, pp. 587–596, 2002.

[6] N. C. Avery, T. J. Sims, and A. J. Bailey, "Quantitative determination of collagen cross-links," *Methods in Molecular Niology*, vol. 522, pp. 103–21, 1 2009.

[7] D. R. Eyre, M. Paz, and P. Gallop, "Cross-linking in collagen and elastin," *Annual review of biochemistry*, vol. 53, pp. 717–48, 1 1984. [Online]. Available: http://www.ncbi.nlm.nih.gov/pubmed/6148038

[8] D. R. Eyre, M. A. Weis, and J.-J. Wu, "Advances in collagen cross-link analysis." *Methods*, vol. 45, no. 1, pp. 65–74, 5 2008.

[9] E. Gineyts, O. Borel, R. Chapurlat, and P. Garnero, "Quantification of immature and mature collagen crosslinks by liquid chromatography-electrospray ionization mass spectrometry in connective tissues," *Journal of Chromatography B: Analytical Technologies in the Biomedical and Life Sciences*, vol. 878, no. 19, pp. 1449–1454, 2010.

[10] M. Saito and K. Marumo, "Collagen cross-links as a determinant of bone quality: a possible explanation for bone fragility in aging, osteoporosis, and diabetes mellitus," *Osteoporosis International*, vol. 21, no. 2, pp. 195–214, 2 2010.

[11] A. Forlino, W. A. Cabral, A. M. Barnes, and J. C. Marini, "New perspectives on osteogenesis imperfecta," *Nature reviews. Endocrinology*, vol. 7, no. 9, pp. 540–57, 9 2011.

[12] F. Rauch and F. H. Glorieux, "Osteogenesis imperfecta," *Lancet*, vol. 363, no. 9418, pp. 1377–85, 4 2004.

[13] B. P. Sinder, M. M. Eddy, M. S. Ominsky, M. S. Caird, J. C. Marini, and K. M. Kozloff, "Sclerostin antibody improves skeletal parameters in a Brtl/+ mouse model of osteogenesis imperfecta," *Journal of bone and mineral research*, vol. 28, no. 1, pp. 73–80, 1 2013. [Online]. Available: http://www.ncbi.nlm.nih.gov/pubmed/22836659

[14] R. A. Bank, J. M. Tekoppele, G. J. Janus, M. H. Wassen, H. E. Pruijs, H. A. Van der Sluijs, and R. J. Sakkers, "Pyridinium Cross-Links in Bone of Patients with Osteogenesis Imperfecta: Evidence of a Normal Intrafibrillar Collagen Packing," *Journal of Bone and Mineral Research*, vol. 15, no. 7, pp. 1330–1336, 7 2000.

[15] U. Vetter, M. A. Weis, M. Mörike, E. Eanes, and D. R. Eyre, "Collagen crosslinks and mineral crystallinity in bone of patients with osteogenesis imperfecta," *Journal of bone and mineral research*, vol. 8, no. 2, pp. 133–7, 2 1993.

[16] M. J. Silva, M. D. Brodt, M. A. Lynch, J. A. McKenzie, K. M. Tanouye, J. S. Nyman, and X. Wang, "Type 1 diabetes in young rats leads to progressive trabecular bone loss, cessation of cortical bone growth, and diminished whole bone strength and fatigue life," *Journal of bone and mineral research*, vol. 24, no. 9, pp. 1618–27, 9 2009.

[17] S. Viguet-Carrin, D. Farlay, Y. Bala, F. Munoz, M. L. Bouxsein, and P. D. Delmas, "An in vitro model to test the contribution of advanced glycation end products to bone biomechanical properties," *Bone*, vol. 42, pp. 139–149, 2008.

[18] S. Viguet-Carrin, J. Roux, M. Arlot, Z. Merabet, D. Leeming, I. Byrjalsen, P. D. Delmas, and M. L. Bouxsein, "Contribution of the advanced glycation end product pentosidine and of maturation of type I collagen to compressive biomechanical properties of human lumbar vertebrae," *Bone*, vol. 39, no. 5, pp. 1073–1079, 2006.

[19] P. Garnero, O. Borel, E. Gineyts, F. Duboeuf, H. Solberg, M. L. Bouxsein, C. Christiansen, and P. D. Delmas, "Extracellular post-translational modifications of collagen are major determinants of biomechanical properties of fetal bovine cortical bone," *Bone*, vol. 38, no. 3, pp. 300–9, 3 2006.

[20] C. J. Hernandez, S. Y. Tang, B. M. Baumbach, P. B. Hwu, A. N. Sakkee, F. Van der Ham, J. DeGroot, R. A. Bank, and T. M. Keaveny, "Trabecular microfracture and the influence of pyridinium and non-enzymatic glycation-mediated collagen cross-links," *Bone*, vol. 37, pp. 825–832, 2005.

[21] X. Banse, T. J. Sims, and A. J. Bailey, "Mechanical properties of adult vertebral cancellous bone: correlation with collagen intermolecular cross-links." *Journal of bone and mineral research*, vol. 17, no. 9, pp. 1621–8, 9 2002. [Online]. Available: http://www.ncbi.nlm.nih.gov/pubmed/12211432

[22] S. Viguet-Carrin, P. Garnero, and P. D. Delmas, "The role of collagen in bone strength," *Osteoporosis international*, vol. 17, no. 3, pp. 319–36, 1 2006. [Online]. Available: http://www.ncbi.nlm.nih.gov/pubmed/16341622

[23] L. Knott and A. J. Bailey, "Collagen biochemistry of avian bone: comparison of bone type and skeletal site," *British poultry science*, vol. 8, no. November 1998, pp. 371–379, 1999.

[24] X. Banse, J. Devogelaer, A. Lafosse, T. J. Sims, M. Grynpas, and A. J. Bailey, "Cross-link profile of bone collagen correlates with structural organization of trabeculae," *Bone*, vol. 31, no. 1, pp. 70–76, 7 2002.

[25] A. Hodge and J. Petruska, "Recent studies with the electron microscope on ordered aggregates of the tropocollagen molecule," in *Aspects of protein structure*, G. M. Ramachandran, Ed., 1963, p. 289.

[26] D. J. Hulmes, A. Miller, D. A. Parry, K. A. Piez, and J. Woodhead-Galloway, "Analysis of the primary structure of collagen for the origins of molecular packing," *Journal of Molecular Biology*, vol. 79, no. 1, pp. 137–148, 1973.

[27] V. Baranauskas, I. Garavello-Freitas, Z. Jingguo, and M. Cruz-Hofling, "Observation of the bone matrix structure of intact and regenerative zones of tibias by atomic force microscopy," *Journal of Vacuum Science & Technology A: Vacuum, Surfaces, and Films*, vol. 19, no. 4, p. 1042, 7 2001. [Online]. Available: http://ieeexplore.ieee.org/articleDetails.jsp?arnumber=4921453

[28] J. Ge, F.-Z. Cui, X. Wang, and Y. Wang, "New evidence of surface mineralization of collagen fibrils in wild type zebrafish skeleton by AFM and TEM," *Materials Science and Engineering*, vol. 27, pp. 46–50, 2007.

[29] M. Balooch, S. Habelitz, J. Kinney, S. J. Marshall, and G. W. Marshall, "Mechanical properties of mineralized collagen fibrils as influenced by demineralization," *Journal of structural biology*, vol. 162, pp. 404–410, 2008.

[30] L. Bozec, J. DeGroot, M. Odlyha, B. Nicholls, and M. A. Horton, "Mineralised tissues as nanomaterials: analysis by atomic force microscopy," *IEE proceedings. Nanobiotechnology*, vol. 152, no. 5, pp. 183–6, 10 2005.

[31] E. A. Chernoff, "Atomic force microscope images of collagen fibers," *Journal of Vacuum Science & Technology A: Vacuum, Surfaces, and Films*, vol. 10, no. 4, p. 596, 7 1992.

[32] T. Hassenkam, H. L. Jørgensen, and J. B. Lauritzen, "Mapping the imprint of bone remodeling by atomic force microscopy," *The anatomical record. Part A, Discoveries in molecular, cellular, and evolutionary biology*, vol. 288, no. 10, pp. 1087–94, 10 2006.

[33] P. J. Thurner, E. Oroudjev, R. Jungmann, C. Kreutz, J. H. Kindt, and G. Schitter, "Imaging of Bone Ultrastructure using Atomic Force Microscopy," *Modern Research and Educational Topics in Microscopy*, pp. 37–48, 2007.

[34] C. Barragan-Adjemian, D. Nicolella, V. Dusevich, M. Dallas, J. Eick, and L. F. Bonewald, "Mechanism by which MLO-A5 late osteoblasts/early osteocytes mineralize in culture: similarities with mineralization of lamellar bone," *Calcified tissue international*, vol. 79, no. 5, pp. 340–53, 11 2006.

[35] L. Bozec, J. d. Groot, M. Odlyha, B. Nicholls, S. Nesbitt, A. Flanagan, and M. A. Horton, "Atomic force microscopy of collagen structure in bone and dentine revealed by osteoclastic resorption," *Ultramicroscopy*, vol. 105, pp. 79–89, 2005.

[36] S. Habelitz, M. Balooch, S. J. Marshall, G. Balooch, and G. W. Marshall, "In situ atomic force microscopy of partially demineralized human dentin collagen fibrils," *Journal of structural biology*, vol. 138, no. 3, pp. 227–36, 6 2002.

[37] T. Hassenkam, G. E. Fantner, J. A. Cutroni, J. C. Weaver, D. E. Morse, and P. K. Hansma, "High-resolution AFM imaging of intact and fractured trabecular bone," *Bone*, vol. 35, no. 1, pp. 4–10, 2004.

[38] J. H. Kindt, P. J. Thurner, M. Lauer, B. Bosma, G. Schitter, G. E. Fantner, M. Izumi, J. C. Weaver, D. Morse, and P. K. Hansma, "In situ observation of fluoride-ion-induced hydroxyapatite-collagen detachment on bone fracture surfaces by atomic force microscopy," *Nanotechnology*, vol. 18, no. 13, p. 135102, 4 2007.

[39] H. F. Knapp, A. Stemmer, G. C. Reilly, P. Niederer, and M. L. Knothe Tate, "Development of preparation methods for and insights obtained from atomic force microscopy of fluid spaces in cortical bone," *Scanning*, vol. 24, no. 1, pp. 25–33, 12 2006. [Online]. Available: http://doi.wiley.com/10.1002/sca.4950240104

[40] N. Sasaki, A. Tagami, T. Goto, M. Taniguchi, M. Nakata, and K. Hikichi, "Atomic force microscopic studies on the structure of bovine femoral cortical bone at the collagen fibril-mineral level," *Journal of Materials Science: Materials in Medicine*, vol. 13, no. 3, pp. 333–337, 3 2002.

[41] J. M. Wallace, B. Erickson, C. M. Les, B. G. Orr, and M. M. Banaszak Holl, "Distribution of type I collagen morphologies in bone: relation to estrogen depletion," *Bone*, vol. 46, no. 5, pp. 1349–54, 5 2010.

[42] J. M. Wallace, B. G. Orr, J. C. Marini, and M. M. Banaszak Holl, "Nanoscale morphology of Type I collagen is altered in the Brtl mouse model of Osteogenesis Imperfecta," *Journal of Structural Biology*, vol. 173, no. 1, pp. 146–52, 1 2011.

[43] A. D. Kemp, C. C. Harding, W. A. Cabral, J. C. Marini, and J. M. Wallace, "Effects of tissue hydration on nanoscale structural morphology and mechanics of individual Type I collagen fibrils in the Brtl mouse model of Osteogenesis Imperfecta," *Journal of structural biology*, vol. 180, no. 3, pp. 428–38, 12 2012.

[44] J. M. Wallace, Q. Chen, M. Fang, B. Erickson, B. G. Orr, and M. M. Banaszak Holl, "Type I collagen exists as a distribution of nanoscale morphologies in teeth, bones, and tendons," *Langmuir*, vol. 26, no. 10, pp. 7349–54, 5 2010.

[45] B. Erickson, M. Fang, J. M. Wallace, B. G. Orr, C. M. Les, and M. M. Banaszak Holl, "Nanoscale structure of type I collagen fibrils: quantitative measurement of D-spacing," *Biotechnology Journal*, vol. 8, no. 1, pp. 117–26, 1 2013.

[46] J. A. Chapman, M. Tzaphlidou, K. M. Meek, and K. E. Kadler, "The collagen fibrilA model system for studying the staining and fixation of a protein," *Electron Microscopy Reviews*, vol. 3, no. 1, pp. 143–182, 1 1990.

[47] P. Fratzl, N. Fratzl-Zelman, and K. Klaushofer, "Collagen packing and mineralization. An x-ray scattering investigation of turkey leg tendon," *Biophysical journal*, vol. 64, no. 1, pp. 260–6, 1 1993.

[48] M. C. Goh, M. Paige, M. Gale, I. Yadegari, M. Edirisinghe, and J. Strzelczyk, "Fibril formation in collagen," *Physica A: Statistical Mechanics and its Applications*, vol. 239, no. 1-3, pp. 95–102, 5 1997.

[49] M. Gale, M. S. Pollanen, P. Markiewicz, and M. C. Goh, "Sequential assembly of collagen revealed by atomic force microscopy," *Biophysical journal*, vol. 68, no. May, pp. 2124–2128, 1995. [Online]. Available: http://www.sciencedirect.com/science/article/pii/S0006349595803930

[50] C. A. Grant, D. J. Brockwell, S. E. Radford, and N. H. Thomson, "Effects of hydration on the mechanical response of individual collagen fibrils," *Applied Physics Letters*, vol. 92, no. 23, p. 233902, 6 2008. [Online]. Available: http://link.aip.org.ezproxy.lib.purdue.edu/link/?APPLAB/92/233902/1

[51] A. Gautieri, S. Vesentini, A. Redaelli, and M. J. Buehler, "Hierarchical structure and nanomechanics of collagen microfibrils from the atomistic scale up," *Nano Letters*, vol. 11, no. 2, pp. 757–66, 2 2011.

[52] L. Cueru, A. Trunfio-Sfarghiu, Y. Bala, B. Depalle, Y. Berthier, and H. Follet, "Mechanical and physicochemical multiscale analysis of cortical bone," *Computer Methods in Biomechanics and Biomedical Engineering*, vol. 14, no. sup1, pp. 223–225, 8 2011. [Online]. Available: http://dx.doi.org/10.1080/10255842.2011.595199

[53] N. Nassif, F. Gobeaux, J. Seto, E. Belamie, P. Davidson, P. Panine, G. Mosser, P. Fratzl, and M.-M. Giraud Guille, "Self-Assembled Collagen-Apatite Matrix with Bone-like Hierarchy," *Chemistry of Materials*, vol. 22, no. 11, pp. 3307–3309, 6 2010. [Online]. Available: http://pubs.acs.org/doi/abs/10.1021/cm903594n

[54] K. Tai, M. Dao, S. Suresh, A. Palazoglu, and C. Ortiz, "Nanoscale heterogeneity promotes energy dissipation in bone," *Nature materials*, vol. 6, no. 6, pp. 454–62, 6 2007.

[55] J. Thompson, J. H. Kindt, B. Drake, H. Hansma, D. Morse, and P. K. Hansma, "Bone indentation recovery time correlates with bond reforming time." *Nature*, vol. 414, no. 6865, pp. 773–6, 12 2001.

[56] T. Gutsmann, G. E. Fantner, J. H. Kindt, M. Venturoni, S. Danielsen, and P. K. Hansma, "Force spectroscopy of collagen fibers to investigate their mechanical properties and structural organization," *Biophysical journal*, vol. 86, no. 5, pp. 3186–93, 5 2004.

[57] H. M. Frost, "Bone "mass" and the "mechanostat": a proposal," *The Anatomical record*, vol. 219, no. 1, pp. 1–9, 9 1987. [Online]. Available: http://www.ncbi.nlm.nih.gov/pubmed/3688455

[58] C. H. Turner, S. J. Warden, T. Bellido, L. I. Plotkin, N. Kumar, I. Jasiuk, J. Danzig, and A. G. Robling, "Mechanobiology of the skeleton," *Science signaling*, vol. 2, no. 68, 1 2009.

[59] C. H. Turner and F. M. Pavalko, "Mechanotransduction and functional response of the skeleton to physical stress: The mechanisms and mechanics of bone adaptation," *Journal of Orthopaedic Science*, vol. 3, no. 6, pp. 346–355, 11 1998.

[60] L. A. Bourret and G. A. Rodan, "The role of calcium in the inhibition of cAMP accumulation in epiphyseal cartilage cells exposed to physiological pressure." *Journal of cellular physiology*, vol. 88, no. 3, pp. 353–61, 7 1976.

[61] G. Van Kampen, J. Veldhuijzen, R. Kuijer, R. Van de Stadt, and C. Schipper, "Cartilage response to mechanical force in high-density chondrocyte cultures," *Arthritis & Rheumatism*, vol. 28, no. 4, pp. 419–424, 4 1985.

[62] C. H. Kim, L. You, C. E. Yellowley, and C. R. Jacobs, "Oscillatory fluid flow-induced shear stress decreases osteoclastogenesis through RANKL and OPG signaling," *Bone*, vol. 39, no. 5, pp. 1043–7, 11 2006.

[63] J. Parkkinen, M. Lammi, R. Inkinen, M. Jortikka, M. Tammi, I. Virtanen, and H. J. Helminen, "Influence of short-term hydrostatic pressure on organization of stress fibers in cultured chondrocytes," *Journal of Orthopaedic Research*, vol. 13, no. 4, pp. 495–502, 7 1995.

[64] J. Yousefian, F. Firouzian, J. Shanfeld, P. Ngan, R. Lanese, and Z. Davidovitch, "A new experimental model for studying the response of periodontal ligament cells to hydrostatic pressure," *American journal of orthodontics and dentofacial orthopedics*, vol. 108, no. 4, pp. 402–9, 10 1995. [Online]. Available: http://www.ncbi.nlm.nih.gov/pubmed/7572852

[65] T. Brown, "Techniques for mechanical stimulation of cells in vitro: a review." *Journal of biomechanics*, vol. 33, no. 1, pp. 3–14, 1 2000. [Online]. Available: http://www.ncbi.nlm.nih.gov/pubmed/10609513

[66] C. T. Brighton, R. S. Fisher, S. E. Levine, J. R. Corsetti, T. M. Reilly, A. S. Landsman, J. L. Williams, and L. E. Thibault, "The Biochemical Pathway Mediating the Proliferative Response of Bone Cells to a Mechanical Stimulus," *The Journal of Bone & Joint Surgery*, vol. 78, no. 9, pp. 1337–47, 9 1996.

[67] K. Imamura, H. Ozawa, T. Hiraide, N. Takahashi, Y. Shibasaki, T. Fukuhara, and T. Suda, "Continuously applied compressive pressure induces bone resorption by a mechanism involving prostaglandin E2 synthesis," *Journal of cellular physiology*, vol. 144, no. 2, pp. 222–8, 8 1990. [Online]. Available: http://www.ncbi.nlm.nih.gov/pubmed/2166056

[68] A. el Haj, S. Minter, S. Rawlinson, R. Suswillo, and L. Lanyon, "Cellular responses to mechanical loading in vitro," *Journal of bone and mineral research*, vol. 5, no. 9, pp. 923–32, 9 1990.

[69] S. Rawlinson, J. Mosley, R. Suswillo, A. Pitsillides, and L. Lanyon, "Calvarial and limb bone cells in organ and monolayer culture do not show the same early responses to dynamic mechanical strain," *Journal of bone and mineral research*, vol. 10, no. 8, pp. 1225–32, 8 1995. [Online]. Available: http://www.ncbi.nlm.nih.gov/pubmed/8585427

[70] D. Kaspar, W. Seidl, C. Neidlinger-Wilke, A. Ignatius, and L. Claes, "Dynamic cell stretching increases human osteoblast proliferation and CICP synthesis but decreases osteocalcin synthesis and alkaline phosphatase activity," *Journal of Biomechanics*, vol. 33, no. 1, pp. 45–51, 1 2000.

[71] D. Kaspar, W. Seidl, A. Ignatius, C. Neidlinger-Wilke, and L. Claes, "In vitro cell behavior of human osteoblasts after physiological dynamic stretching," *Orthopäde*, vol. 29, no. 2, pp. 85–90, 2 2000.

[72] D. Murray and N. Rushton, "The effect of strain on bone cell prostaglandin E2 release: A new experimental method," *Calcified Tissue International*, vol. 47, no. 1, pp. 35–39, 7 1990.

[73] D. Jones, H. Nolte, J.-G. Scholübbers, E. Turner, and D. Veltel, "Biochemical signal transduction of mechanical strain in osteoblast-like cells," *Biomaterials*, vol. 12, no. 2, pp. 101–110, 1991.

[74] A. Pitsillides, S. Rawlinson, R. Suswillo, S. Bourrin, G. Zaman, and L. Lanyon, "Mechanical strain-induced NO production by bone cells: a possible role in adaptive bone (re)modeling?" *FASEB Journal*, vol. 9, no. 15, pp. 1614–1622, 12 1995.

[75] S. Hasegawa, S. Sato, S. Saito, Y. Suzuki, and D. Brunette, "Mechanical stretching increases the number of cultured bone cells synthesizing DNA and alters their pattern of protein synthesis," *Calcified Tissue International*, vol. 37, no. 4, pp. 431–436, 7 1985.

[76] T. Matsuo, H. Uchida, and N. Matsuo, "Bovine and porcine trabecular cells produce prostaglandin F2 alpha in response to cyclic mechanical stretching." *Japanese journal of ophthalmology*, vol. 40, no. 3, pp. 289–96, 1 1996. [Online]. Available: http://europepmc.org/abstract/MED/8988417/reload=0

[77] S. Soma, S. Matsumoto, and T. Takano-Yamamoto, "Enhancement by conditioned medium of stretched calvarial bone cells of the osteoclast-like cell formation induced by parathyroid hormone in mouse bone marrow cultures," *Archives of Oral Biology*, vol. 42, no. 3, pp. 205–211, 1997.

[78] A. J. Banes, J. Gilbert, D. Taylor, and O. Monbureau, "A new vacuum-operated stress-providing instrument that applies static or variable duration cyclic tension or compression to cells in vitro," *J. Cell Sci.*, vol. 75, no. 1, pp. 35–42, 4 1985. [Online]. Available: http://jcs.biologists.org/content/75/1/35.short

[79] C. Brighton, B. Strafford, S. Gross, D. Leatherwood, J. Williams, and S. Pollack, "The proliferative and synthetic response of isolated calvarial bone cells of rats to cyclic biaxial mechanical strain," *The Journal of Bone & Joint Surgery*, vol. 73, no. 3, pp. 320–331, 3 1991. [Online]. Available: http://jbjs.org/article.aspx?articleid=21570

[80] J. Schaffer, M. Rizen, G. L'Italien, A. Benbrahim, J. Megerman, L. C. Gerstenfeld, and M. Gray, "Device for the application of a dynamic biaxially uniform and isotropic strain to a flexible cell culture membrane," *Journal of orthopaedic research*, vol. 12, no. 5, pp. 709–19, 9 1994. [Online]. Available: http://www.ncbi.nlm.nih.gov/pubmed/7931788

[81] M. J. Buckley, A. J. Banes, and R. D. Jordan, "The effects of mechanical strain on osteoblasts in vitro," *Journal of Oral and Maxillofacial Surgery*, vol. 48, no. 3, pp. 276–282, 1990.

[82] X. Liu, X. Zhang, and Z.-P. Luo, "Strain-related collagen gene expression in human osteoblast-like cells." *Cell and tissue research*, vol. 322, no. 2, pp. 331–4, 11 2005. [Online]. Available: http://www.ncbi.nlm.nih.gov/pubmed/16133149

[83] L. Tang, Z. Lin, and Y.-m. Li, "Effects of different magnitudes of mechanical strain on osteoblasts in vitro," *Biochemical and Biophysical Research Communications*, vol. 344, no. 1, pp. 122–128, 2006. [Online]. Available: http://www.sciencedirect.com/science/article/pii/S0006291X06006760

[84] K. Ziambaras, F. Lecanda, T. Steinberg, and R. Civitelli, "Cyclic stretch enhances gap junctional communication between osteoblastic cells," *Journal of bone and mineral research*, vol. 13, no. 2, pp. 218–28, 2 1998.

[85] L. A. Norton, K. L. Andersen, D. Arenholt-Bindslev, L. Andersen, and B. Melsen, "A methodical study of shape changes in human oral cells perturbed by a simulated orthodontic strain in vitro," *Archives of Oral Biology*, vol. 40, no. 9, pp. 863–872, 1995.

[86] K. Sakai, M. Mohtai, and Y. Iwamoto, "Fluid Shear Stress Increases Transforming Growth Factor Beta 1 Expression in Human Osteoblast-like Cells: Modulation by Cation Channel Blockades," *Calcified Tissue International*, vol. 63, no. 6, pp. 515–520, 12 1998. [Online]. Available: http://link.springer.com/10.1007/s002239900567

[87] C. T. Hung, S. Pollack, T. M. Reilly, C. T. Brighton, S. R. Polllack, T. M. Reilly, and C. T. Brighton, "Real-time calcium response of cultured bone cells to fluid flow," *Clinical orthopaedics and related research*, vol. 313, pp. 256–269, 4 1995. [Online]. Available: http://www.ncbi.nlm.nih.gov/pubmed/7641488

[88] C. R. Jacobs, C. E. Yellowley, B. Davis, Z. Zhou, J. Cimbala, and H. J. Donahue, "Differential effect of steady versus oscillating flow on bone cells." *Journal of biomechanics*, vol. 31, no. 11, pp. 969–76, 11 1998.

[89] M. J. Barron, C.-J. Tsai, and S. W. Donahue, "Mechanical stimulation mediates gene expression in MC3T3 osteoblastic cells differently in 2D and 3D environments." *Journal of biomechanical engineering*, vol. 132, no. 4, p. 041005, 4 2010. [Online]. Available: http://www.ncbi.nlm.nih.gov/pubmed/20387968

[90] W. S. Van Dyke, X. Sun, A. B. Richard, E. A. Nauman, and O. Akkus, "Novel mechanical bioreactor for concomitant fluid shear stress and substrate strain." *Journal of biomechanics*, vol. 45, no. 7, pp. 1323–7, 4 2012.

[91] A. G. Robling, A. B. Castillo, and C. H. Turner, "Biomechanical and molecular regulation of bone remodeling," *Annual review of biomedical engineering*, vol. 8, pp. 455–498, 7 2006.

[92] M. Saunders, J. You, J. Trosko, H. Yamasaki, Z. Li, H. J. Donahue, and C. R. Jacobs, "Gap junctions and fluid flow response in MC3T3-E1 cells," *Am J Physiol Cell Physiol*, vol. 281, no. 6, pp. 1917–1925, 12 2001.

[93] K. Sawakami, A. G. Robling, M. Ai, N. D. Pitner, D. Liu, S. J. Warden, J. Li, P. Maye, D. W. Rowe, R. L. Duncan, M. L. Warman, and C. H. Turner, "The Wnt co-receptor LRP5 is essential for skeletal mechanotransduction but not for the anabolic bone response to parathyroid hormone treatment." *The Journal of biological chemistry*, vol. 281, no. 33, pp. 23 698–711, 8 2006.

[94] H. Zhou, A. B. Newnum, J. R. Martin, P. Li, M. T. Nelson, A. Moh, X.-Y. Fu, H. Yokota, and J. Li, "Osteoblast/osteocyte-specific inactivation of Stat3 decreases load-driven bone formation and accumulates reactive oxygen species," *Bone*, vol. 49, no. 3, pp. 404–11, 9 2011. [Online]. Available: http://dx.doi.org/10.1016/j.bone.2011.04.020

[95] D. Liu, D. C. Genetos, Y. Shao, D. J. Geist, J. Li, H. Z. Ke, C. H. Turner, and R. L. Duncan, "Activation of extracellular-signal regulated kinase (ERK1/2) by fluid shear is Ca(2+)- and ATP-dependent in MC3T3-E1 osteoblasts," *Bone*, vol. 42, no. 4, pp. 644–52, 4 2008.

[96] L. A. Sharp, Y. W. Lee, and A. S. Goldstein, "Effect of low-frequency pulsatile flow on expression of osteoblastic genes by bone marrow stromal cells." *Annals of biomedical engineering*, vol. 37, no. 3, pp. 445–53, 3 2009. [Online]. Available: http://www.ncbi.nlm.nih.gov/pubmed/19130228

[97] C.-C. Wu, Y.-S. Li, J. H. Haga, N. Wang, I. Y.-Z. Lian, F.-C. Su, S. Usami, and S. Chien, "Roles of MAP kinases in the regulation of bone matrix gene expressions in human osteoblasts by oscillatory fluid flow," *Journal of cellular biochemistry*, vol. 98, no. 3, pp. 632–41, 6 2006.

[98] C. Neidlinger-Wilke, H. J. Wilke, and L. Claes, "Cyclic stretching of human osteoblasts affects proliferation and metabolism: a new experimental method and its application." *Journal of orthopaedic research : official publication of the Orthopaedic Research Society*, vol. 12, no. 1, pp. 70–8, 1 1994. [Online]. Available: http://www.ncbi.nlm.nih.gov/pubmed/8113944

[99] C.-H. Huang, M.-H. Chen, T.-H. Young, J.-H. Jeng, and Y.-J. Chen, "Interactive effects of mechanical stretching and extracellular matrix proteins on initiating osteogenic differentiation of human mesenchymal stem cells." *Journal of cellular biochemistry*, vol. 108, no. 6, pp. 1263–73, 12 2009. [Online]. Available: http://www.ncbi.nlm.nih.gov/pubmed/19795386

[100] M. Wozniak, A. Fausto, C. Carron, D. Meyer, and K. Hruska, "Mechanically strained cells of the osteoblast lineage organize their extracellular matrix through unique sites of alphavbeta3-integrin expression." *Journal of bone and mineral research : the official journal of the American Society for Bone and Mineral Research*, vol. 15, no. 9, pp. 1731–45, 9 2000. [Online]. Available: http://www.ncbi.nlm.nih.gov/pubmed/10976993

[101] D. Huang, T. R. Chang, A. Aggarwal, R. C. Lee, and H. P. Ehrlich, "Mechanisms and dynamics of mechanical strengthening in ligament-equivalent fibroblast-populated collagen matrices," *Annals of Biomedical Engineering*, vol. 21, no. 3, pp. 289–305, 5 1993. [Online]. Available: http://link.springer.com/10.1007/BF02368184

[102] D. B. Burr and M. R. Allen, *Basic and Applied Bone Biology*, 1st ed., D. Burr and M. Allen, Eds. San Diego, CA: Elsevier, 2013.

[103] A. L. Boskey, T. Wright, and R. Blank, "Collagen and bone strength," *Journal of bone and mineral research*, vol. 14, no. 3, pp. 330–335, 1999. [Online]. Available: http://onlinelibrary.wiley.com/doi/10.1359/jbmr.1999.14.3.330/full

[104] D. B. Burr, "The contribution of the organic matrix to bones material properties," *Bone*, vol. 31, no. 1, pp. 8–11, 7 2002. [Online]. Available: http://www.sciencedirect.com/science/article/pii/S8756328202008153

[105] S. R. Cummings, J. L. Kelsey, M. C. Nevitt, and K. J. O'Dowd, "Epidemiology of osteoporosis and osteoporotic fractures," *Epidemiologic reviews*, vol. 7, 1985.

[106] S. Becker and M. Ogon, "Epidemiology of osteoporosis," *Balloon Kyphoplasty*, vol. 16, no. 5, pp. 1–3, 2008.

[107] WHO, "Assessment of fracture risk and its application to screening for postmenopausal osteoporosis: Report of a WHO study group," *World Health Organization Technical Report Series*, vol. 843, no. 1, 1994.

[108] K. Jepsen, M. Schaffler, J. Kuhn, R. Goulet, J. Bonadio, and S. Goldstein, "Type I collagen mutation alters the strength and fatigue behavior of Mov13 cortical tissue." *Journal of biomechanics*, vol. 30, no. 11-12, pp. 1141–7, 1997. [Online]. Available: http://www.ncbi.nlm.nih.gov/pubmed/9456382

[109] P. Byers, G. Wallis, and M. Willing, "Osteogenesis imperfecta: translation of mutation to phenotype," *Journal of medical genetics*, vol. 28, pp. 433–442, 1991.

[110] K. E. Kadler, D. F. Holmes, J. A. Trotter, and J. A. Chapman, "Collagen fibril formation," *The Biochemical journal*, vol. 316, pp. 1–11, 5 1996.

[111] S. P. Canelón and J. M. Wallace, "β-Aminopropionitrile-Induced Reduction in Enzymatic Crosslinking Causes In Vitro Changes in Collagen Morphology and Molecular Composition," *PLOS ONE*, vol. 11, no. 11, pp. 1–13, 11 2016.

[112] D. R. Eyre and J.-J. Wu, "Collagen Cross-Links," *Top Curr Chem*, vol. 247, pp. 207–229, 1 2005.

[113] W. Dasler, "Isolation of toxic crystals from sweet peas (Lathyrus odoratus)," *Science*, vol. 120, no. 3112, pp. 307–308, 1954.

[114] M. E. Nimni, "Mechanism of inhibition of collagen crosslinking by penicillamine," *Proceedings of the Royal Society of Medicine*, vol. 70 Suppl 3, no. Suppl 3, pp. 65–72, 1 1977.

[115] R. Siegel, "Collagen cross-linking. Synthesis of collagen cross-links in vitro with highly purified lysyl oxidase." *J. Biol. Chem.*, vol. 251, no. 18, pp. 5786–5792, 9 1976.

[116] E. M. McNerny, B. Gong, M. D. Morris, and D. H. Kohn, "Bone fracture toughness and strength correlate with collagen cross-link maturity in a dose-controlled lathyrism mouse model," *Journal of Bone and Mineral Research*, vol. 30, no. 3, pp. 455–464, 2015.

[117] S. Lees, D. Hanson, E. Page, and H. A. Mook, "Comparison of dosage-dependent effects of beta-aminopropionitrile, sodium fluoride, and hydrocortisone on selected physical properties of cortical bone," *Journal of Bone and Mineral Researchineral research*, vol. 9, no. 9, pp. 1377–89, 9 1994.

[118] E. P. Paschalis, D. Tatakis, S. Robins, P. Fratzl, I. Manjubala, R. Zoehrer, S. Gamsjaeger, B. Buchinger, A. Roschger, R. J. Phipps, A. L. Boskey, E. Dall'Ara, P. Varga, P. Zysset, K. Klaushofer, and P. Roschger, "Lathyrism-induced alterations in collagen cross-links influence the mechanical properties of bone material without affecting the mineral," *Bone*, vol. 49, no. 6, pp. 1232–1241, 2011.

[119] H. Fernandes, "The role of collagen crosslinking in differentiation of human mesenchymal stem cells and MC3T3-E1 cells," *Tissue Engineering Part A*, vol. 15, no. 12, 2009.

[120] R. Thaler, S. Spitzer, M. Rumpler, N. Fratzl-Zelman, K. Klaushofer, E. Paschalis, and F. Varga, "Differential effects of homocysteine and beta aminopropionitrile on preosteoblastic MC3T3-E1 cells," *Bone*, vol. 46, no. 3, pp. 703–709, 3 2010.

[121] C. Turecek, N. Fratzl-Zelman, M. Rumpler, B. Buchinger, S. Spitzer, R. Zoehrer, E. Durchschlag, K. Klaushofer, E. Paschalis, and F. Varga, "Collagen cross-linking influences osteoblastic differentiation." *Calcified tissue international*, vol. 82, no. 5, pp. 392–400, 5 2008.

[122] H. Fernandes, K. Dechering, E. Van Someren, C. Van Blitterswijk, and J. de Boer, "Investigating the role of the extracellular matrix on differentiation of human mesenchymal stem cells and MC3T3 cells," in *Bone*, vol. 42, 3 2008, p. S21. [Online]. Available: http://www.sciencedirect.com/science/article/pii/S875632820700912X

[123] A. D. Gonzalez, M. A. Gallant, D. B. Burr, and J. M. Wallace, "Multiscale analysis of morphology and mechanics in tail tendon from the ZDSD rat model of type 2 diabetes," *Journal of biomechanics*, vol. 47, no. 3, pp. 681–6, 2 2014.

[124] J. M. Wallace, K. Golcuk, M. D. Morris, and D. H. Kohn, "Inbred strain-specific response to biglycan deficiency in the cortical bone of C57BL6/129 and C3H/He mice." *Journal of Bone and Mineral Research Research*, vol. 24, no. 6, pp. 1002–12, 6 2009.

[125] T. D. Schmittgen and B. A. Zakrajsek, "Effect of experimental treatment on housekeeping gene expression: validation by real-time, quantitative RT-PCR," *Journal of Biochemical and Biophysical Methods*, vol. 46, no. 1-2, pp. 69–81, 11 2000.

[126] M. W. Pfaffl, "A new mathematical model for relative quantification in real-time RT-PCR," *Nucleic Acids Research*, vol. 29, no. 9, pp. 45e–45, 5 2001.

[127] M. W. Pfaffl, G. W. Horgan, and L. Dempfle, "Relative expression software tool (REST(C)) for group-wise comparison and statistical analysis of relative expression results in real-time PCR," *Nucleic Acids Research*, vol. 30, no. 9, pp. 36e–36, 5 2002.

[128] H. Yang, S. Yang, J. Kong, A. Dong, and S. Yu, "Obtaining information about protein secondary structures in aqueous solution using Fourier transform IR spectroscopy," *Nature Protocols*, vol. 10, no. 3, pp. 382–396, 2015.

[129] A. Dong, P. Huang, and W. S. Caughey, "Protein secondary structures in water from second-derivative amide I infrared spectra." *Biochemistry*, vol. 29, pp. 3303–3308, 1990.

[130] E. Paschalis, K. Verdelis, S. B. Doty, A. L. Boskey, R. Mendelsohn, and M. Yamauchi, "Spectroscopic characterization of collagen cross-links in bone," *Journal of Bone and Mineral Research*, vol. 16, no. 10, pp. 1821–8, 10 2001. [Online]. Available: http://www.ncbi.nlm.nih.gov/pubmed/11585346

[131] E. Paschalis, S. Gamsjaeger, D. Tatakis, N. Hassler, S. Robins, and K. Klaushofer, "Fourier transform infrared spectroscopic characterization of mineralizing type I collagen enzymatic trivalent cross-links," *Calcified tissue international*, vol. 96, no. 1, pp. 18–29, 11 2014. [Online]. Available: http://www.ncbi.nlm.nih.gov/pubmed/25424977

[132] M. A. Hammond, A. G. Berman, R. Pacheco-Costa, H. M. Davis, L. I. Plotkin, and J. M. Wallace, "Removing or truncating connexin 43 in murine osteocytes alters cortical geometry, nanoscale morphology, and tissue mechanics in the tibia," *Bone*, vol. 88, pp. 85–91, 2016.

[133] F. Varga, M. Rumpler, R. Zoehrer, C. Turecek, S. Spitzer, R. Thaler, E. Paschalis, and K. Klaushofer, "T3 affects expression of collagen I and collagen cross-linking in bone cell cultures," *Biochemical and Biophysical Research Communications*, vol. 402, no. 2, pp. 180–5, 11 2010. [Online]. Available: http://www.sciencedirect.com/science/article/pii/S0006291X10015081

[134] D. Farlay, M.-E. Duclos, E. Gineyts, C. Bertholon, S. Viguet-Carrin, J. Nallala, G. D. Sockalingum, D. Bertrand, T. Roger, D. J. Hartmann, R. Chapurlat, and G. Boivin, "The ratio 1660/1690 cm(-1) measured by infrared microspectroscopy is not specific of enzymatic collagen cross-links in bone tissue." *PloS One*, vol. 6, no. 12, 1 2011.

[135] D. M. Byler and H. Susi, "Examination of the Secondary Structure of Proteins by Deconvolved FTIR Spectra."

[136] Y. A. Lazarev and A. Lazareva, "Infrared spectra and structure of synthetic polytripeptides," *Biopolymers*, vol. 17, pp. 1197–1214, 1978.

[137] M. A. Hammond and J. M. Wallace, "Exercise prevents β-aminopropionitrile-induced morphological changes to type I collagen in murine bone," *BoneKEy Reports*, vol. 4, no. October 2014, p. 645, 2015. [Online]. Available: http://www.nature.com/doifinder/10.1038/bonekey.2015.12

[138] N. Nagan, P. Callery, and H. Kagan, "Aminoalkylaziridines as substrates and inhibitors of lysyl oxidase: specific inactivation of the enzyme by N-(5-aminopentyl)aziridine," *Frontiers in Bioscience*, vol. 3, no. 22, pp. a23–a26, 1998.

[139] P. Trackman and H. Kagan, "Nonpeptidyl amine inhibitors are substrates of lysyl oxidase," *Journal of Biological Chemistry*, vol. 254, no. 16, pp. 7831–7836, 1979.

[140] J. M. Wallace, "Effects of fixation and demineralization on bone collagen D-spacing as analyzed by atomic force microscopy," *Connective Tissue Research*, pp. 1–8, 1 2015. [Online]. Available: http://informahealthcare.com/doi/abs/10.3109/03008207.2015.1005209

[141] L. C. Gerstenfeld, S. Chipman, C. Kelly, K. Hodgens, D. Lee, and W. Landis, "Collagen expression, ultrastructural assembly, and mineralization in cultures of chicken embryo osteoblasts," *The Journal of Cell Biology*, vol. 106, no. 3, pp. 979–89, 3 1988.

[142] E. P. Paschalis, E. Shane, G. Lyritis, G. Skarantavos, R. Mendelsohn, and A. L. Boskey, "Bone fragility and collagen cross-links," *Journal of bone and mineral research*, vol. 19, no. 12, pp. 2000–4, 12 2004.

[143] J. Peng, Z. Jiang, G. Qin, Q. Huang, Y. Li, Z. Jiao, F. Zhang, Z. Li, J. Zhang, Y. Lu, X. Liu, and J. Liu, "Impact of activity space on the reproductive behaviour of giant panda (Ailuropoda melanoleuca) in captivity," *Applied Animal Behaviour Science*, vol. 104, no. 1-2, pp. 151–161, 1 2007.

[144] R. A. Norris, B. Damon, V. Mironov, V. Kasyanov, A. Ramamurthi, R. Moreno-Rodriguez, T. Trusk, J. D. Potts, R. L. Goodwin, J. Davis, S. Hoffman, X. Wen, Y. Sugi, C. B. Kern, C. H. Mjaatvedt, D. K. Turner, T. Oka, S. J. Conway, J. D. Molkentin, G. Forgacs, and R. R. Markwald, "Periostin regulates collagen fibrillogenesis and the biomechanical properties of connective tissues," *Journal of cellular biochemistry*, vol. 101, no. 3, pp. 695–711, 6 2007.

[145] T. Maruhashi, I. Kii, M. Saito, and A. Kudo, "Interaction between Periostin and BMP-1 Promotes Proteolytic Activation of Lysyl Oxidase," *Journal of Biological Chemistry*, vol. 285, no. 17, pp. 13 294–13 303, 4 2010.

[146] B. Fogelgren, N. Polgár, K. M. Szauter, Z. Újfaludi, R. Laczkó, K. S. Fong, and K. Csiszar, "Cellular Fibronectin Binds to Lysyl Oxidase with High Affinity and Is Critical for Its Proteolytic Activation," *Journal of Biological Chemistry*, vol. 280, no. 26, pp. 24 690–24 697, 7 2005.

[147] L. D. Quarles, D. a. Yohay, L. W. Lever, R. Caton, and R. J. Wenstrup, "Distinct proliferative and differentiated stages of murine MC3T3-E1 cells in culture: an in vitro model of osteoblast development." *Journal of bone and mineral research*, vol. 7, no. 6, pp. 683–92, 6 1992.

[148] D. F. Ward, R. M. Salasznyk, R. F. Klees, J. Backiel, P. Agius, K. Bennett, A. Boskey, and G. E. Plopper, "Mechanical strain enhances extracellular matrix-induced gene focusing and promotes osteogenic differentiation of human mesenchymal stem cells through an extracellular-related kinase-dependent pathway." *Stem cells and development*, vol. 16, no. 3, pp. 467–80, 6 2007. [Online]. Available: http://online.liebertpub.com/doi/abs/10.1089/scd.2007.0034

[149] S. J. Warden, M. R. Galley, A. L. Hurd, J. M. Wallace, M. a. Gallant, J. S. Richard, and L. a. George, "Elevated mechanical loading when young provides lifelong benefits to cortical bone properties in female rats independent of a surgically induced menopause." *Endocrinology*, vol. 154, no. 9, pp. 3178–87, 9 2013. [Online]. Available: http://www.ncbi.nlm.nih.gov/pubmed/23782938http://endo.endojournals.org.proxy.medlib.iupui.edu/content/154/9/3178.long

[150] J. P. Vande Geest, E. S. Di Martino, and D. A. Vorp, "An analysis of the complete strain field within Flexercell(TM) membranes," *Journal of Biomechanics*, vol. 37, no. 12, pp. 1923–1928, 2004.

VITA

SILVIA P. CANELÓN

EDUCATION

Doctorate in Biomedical Engineering *August 2012 – May 2018*
Purdue University – West Lafayette – College of Engineering *West Lafayette, Indiana*

· Dissertation: Characterization of Type I Collagen and Osteoblast Response to Mechanical Loading

Bachelor in Biomedical Engineering *August 2008 – May 2012*
University of Minnesota – Twin Cities – College of Science and Engineering *Minneapolis, Minnesota*

· Senior design project – Team Leader: Create a long-standing treatment for frontal chronic rhinosinusitis using biodesign methodology

RELEVANT COURSEWORK

Graduate
Basic Bone Biology
Biomedical Entrepreneurship
Biomedical Fluid Dynamics
Cellular Mechanotransduction
Continuum Models in Biomedical Engineering
Design of Experiments
Human Motion Kinetics
Introduction to Confocal Microscopy
Linear Algebra with Applications
Quantitative Physiology
Tissue Engineering

Undergraduate
Advanced Biomaterials
Advanced Biomechanics
Advanced Cardiac Physiology and Anatomy
Bioelectricity and Bioinstrumentation
Biomedical Engineering Design
Biomedical Systems Analysis
Biomedical Thermodynamics
Biomedical Transport Processes
Clinical Physiology I
Deformable Body Mechanics
The Healthcare Marketplace

RESEARCH EXPERIENCE

Graduate Research Assistant *May 2012 – May 2018*
Indiana University-Purdue University at Indianapolis *Indianapolis, Indiana*
Principal Investigator: Joseph M. Wallace *Bone Biology and Mechanics Lab*

· Characterized the type I collagen matrix produced by osteoblasts *in vitro* to assess structural, biochemical, mechanical, and biological properties. Assays used include atomic force microscopy, nanoindentation, Fourier transform infrared spectroscopy, and quantitative gene expression analysis.
· Investigated the effect of (1) an induced reduction in molecular crosslinking on type I collagen matrix properties and (2) mechanical loading via equibiaxial substrate strain.

Undergraduate Researcher *June 2010 – May 2012*
University of Minnesota *Minneapolis, Minnesota*
Principal Investigator: David J. Nuckley *Musculoskeletal Biomechanics Research Lab*

· Examined the way in which forces can be applied most optimally to pedicle screws during derotation of a scoliotic spine in order to avoid breaching of vertebral structures during corrective surgery.
· Investigated the correlation between bone mineral density and the force required to cause screw displacement, and link this relationship to the insertional torque of the pedicle screw observed at the screw-bone interface.
· Research resulted in a conference poster presentation (ORS 2013).

Undergraduate Researcher *February 2010 – August 2010*
University of Minnesota *Minneapolis, Minnesota*
Advisor: Marie Johnson *Medical Devices Center*

· Investigated the bactericidal effects and trajectory of ultraviolet light down a polymer sleeve to ultimately surround a central-line catheter.
· Assisted in the modification of the prototype for a biomedical device with the purpose of engineering a more effective model designed to decrease the prevalence of central-line catheter-related bloodstream infections.

INDUSTRY EXPERIENCE

Biomedical Engineering Intern *September 2011 – May 2012*
Medtronic, Inc. – Cardiac Rhythm Disease Management *Mounds View, Minnesota*
Manager: Steve Valley

· Characterized a new thermal bond process on a next generation defibrillator lead.
· Assembled detailed portfolio of thermal bonding processes used within Leads Assembly Engineering.
· Determined benefits and best practices of Pilot Engineering from an academic/industry perspective.

Biomedical Engineering Summer Associate *May 2011 – September 2011*
Medtronic, Inc. – Cardiac Rhythm Disease Management *Mounds View, Minnesota*
Manager: Steve Valley

· Advanced the characterization of a new thermal bond manufacturing process on a next generation defibrillator lead.
· Analyzed torque data from active fix defibrillator being tested for residual torque and helix extension/retraction.
· MDT Summer Associate Technical Project Fair co-chair Planned and coordinated a poster presentation fair of 40 intern presenters from various engineering backgrounds and work groups.
· MDT College Night Registration & Set-Up Committee member Assisted in the planning of a college fair with 400+ attendees; monitored and coordinated the registration of attendees arriving to the event.

SKILLS

Laboratory
Atomic force microscopy
Cellular mechanical loading
Collagen characterization
Fourier Transform infrared spectroscopy
Nanoindentation
Reverse Transcription Polymerase Chain Reaction

Language
English (bilingual)
Spanish (bilingual)

Computer
Adobe Suite
GRAMS/AI
GraphPad Prism
Gwyddion
MATLAB
Microsoft Office
Nanoscope
OriginPro
Scanning Probe Image Software
Statistical Analysis Software

PUBLICATIONS

· **Canelón, S.P.** and Wallace, J.M. β-aminopropionitrile-induced reduction in enzymatic crosslinking causes *in vitro* changes in collagen morphology and molecular composition. PLOS ONE 11(11): 2016.

PRESENTATIONS

· Canelón, S.P. and Wallace, J.M. (2017, June). *Dose-Dependent Effects of Beta-Aminopropionitrile on Osteoblast Gene Expression and Collagen Production.* Poster presented at the Summer Biomechanics, Bioengineering and Biotransport Conference, Tucson, AZ, June 22, 2017.

· Canelón, S.P. and Wallace, J.M. (2015, October). *β-Aminopropionitrile Treatment Effects on MC3T3-E1 Osteoblast Gene Expression and Type I Collagen Production.* Poster presented at the IUPUI Nanotechnology Research Forum and Poster Symposium, Indianapolis, IN, October 23, 2015.

· Canelón, S.P. and Wallace, J.M. (2015, October). *β-Aminopropionitrile Treatment Effects on MC3T3-E1 Osteoblast Gene Expression and Type I Collagen Production.* Poster presented at the American Society for Bone and Mineral Research Annual Meeting, Seattle, WA, October 11, 2015.

· Canelón, S.P. and Wallace, J.M. (2014, October). *Influence of β-Aminopropionitrile on Morphology of Type I Collagen Produced by MC3T3-E1 Osteoblasts and Measured Using Atomic Force Microscopy.* Poster presented at the IUPUI Nanotechnology Research Forum and Poster Symposium, Indianapolis, IN, October 24, 2014.

· Canelón, S.P. and Wallace, J.M. (2014, September). *Influence of β-Aminopropionitrile on Morphology of Type I Collagen Produced by MC3T3-E1 Osteoblasts and Measured Using Atomic Force Microscopy.* Poster presented at the American Society for Bone and Mineral Research Annual Meeting, Houston, TX, September 12, 2014.

· Canelón, S.P., Merkling, S.M., Polly, D.W., Yson, S.C., Sembrano, J.N., and Nuckley, D.J. (2013, January). *Biomechanics of Pedicle Screw Fixation Under Simulated Scoliosis Derotation Surgical Loads.* Poster presented at the Orthopaedic Research Society Annual Meeting, San Antonio, TX, January 26, 2013.

AWARDS

· Stephen R. Ash Fellowship – Weldon School of Biomedical Engineering (Jan. 2018)

· Purdue Research Foundation Doctoral Research Award – Purdue University (May 2016)

· Elite 50 Graduate School Award – Indiana University-Purdue University at Indianapolis (April 2015)

· Joe Bourland Graduate Student Travel Award – Weldon School of Biomedical Engineering (Oct. 2014)

· Boston Scientific Scholarship – Minnesota Section of the Society of Women Engineers (May 2011)

LEADERSHIP

Barter School Indy *May 2016 – April 2017*
Rabble Coffee *Indianapolis, Indiana*

- **Board Member** – Provided expertise in an advisory capacity on a board of 4 former Trade School organizers to ensure smooth transitions and continuity between semesters.
- **Summer Communications Organizer** – Served as the point of contact between the Trade School Indianapolis cooperative and the community, including students, teachers, and 165 co-op members.

Graduate & Professional Student Government *April 2013 – August 2015*
Indiana University-Purdue University at Indianapolis *Indianapolis, Indiana*

- **Supreme Court of Student Governance Chief Justice** – Managed the judicial branch of student government at IUPUI comprised of an additional three graduate/professional justices and three undergraduate justices (January 2014 – August 2015).
    - Served as student representative to the IUPUI University Hearing Commission to hear student misconduct appeals received by the University Office of Student Conduct regarding Student Conduct Code violations occurring on the IUPUI campus or relating to its student body.
    - Interpreted the Constitution and contractual agreements of both the Graduate & Professional Student and Undergraduate Student Governments and addressed issues relating to legislation, executive decisions, removal procedures, hearings, and the relationship between both student governments.
- **Graduate-Professional Enhancement Grant Committee Member** – Reviewed and scored 50+ applications received from IUPUI students for funding of travel, training, or research materials.

Biomedical Engineering Graduate Student Association *May 2013 – April 2014*
Indiana University-Purdue University at Indianapolis *Indianapolis, Indiana*

- **Secretary** – Served as the main point of contact between the Officers and the general student body, maintained record of Officer meetings, distributed information to general body as needed to serve the organizations mission, and served as representative to the Graduate & Professional Student Government.

Biomedical Engineering Graduate Student Association *September 2012 – April 2013*
Purdue University *West Lafayette, Indiana*

- **First Year Representative** – Served as first-year graduate student liaison to the Weldon School of Biomedical Engineering graduate student association, which included encouraging attendance at general body meetings and programmed events as well as serving as Team Captain for the Schools 2013 Relay for Life team.

Society of Women Engineers *September 2008 – May 2012*
University of Minnesota *Minneapolis, Minnesota*

- **Co-Director of Corporate Relations** – Maintained professional relationships with company representatives and ensured their communication with the members of the chapter via monthly meetings and/or informational sessions (May 2011 – May 2012).
- **Co-Director of the Science and Engineering Career Fair** – Efficiently planned and organized the largest career fair within the Colleges of Science & Engineering and Biological Sciences by overseeing the registration procedure, managing secretarial duties, and establishing relationships with attending companies (May 2010 – May 2011).

Society of Women Engineers – National *August 2011 – May 2012*

- **Co-Director of Corporate Relations** – Maintained professional relationships with company representatives and ensured their communication with the members of the chapter via monthly meetings and/or informational sessions (May 2011 – May 2012).
- **Co-Director of the Science and Engineering Career Fair** – Efficiently planned and organized the largest career fair within the Colleges of Science & Engineering and Biological Sciences by overseeing the registration procedure, managing secretarial duties, and establishing relationships with attending companies (May 2010 – May 2011).

Senate Committee of Student Affairs *May 2010 – May 2012*
University of Minnesota *Minneapolis, Minnesota*

- **Co-Chair** – Formulated and recommended policies to the Senate pertaining to all student affairs and provide a comprehensive link between the University and the student body.
- **Student Representative** (January 2009 – May 2010)

Regent Candidate Advisory Council *June 2010 – May 2012*
Office of the Secretary of State *Saint Paul, Minnesota*

- **Student Representative** – Advised the legislature in the election of members to the University of Minnesotas Board of Regents based on a comprehensive evaluation of how candidate qualifications met criteria integral to the success of the University.

Office for Student Affairs, Student Advisory Board *August 2009 – May 2011*
University of Minnesota *Minneapolis, Minnesota*

- **At-Large Member** – Provided advice to the Vice Provost for Student Affairs regarding the student experience outside of the classroom and discussed topics which impacted the student experience.